THE REACTIONS OF VARIOUS RUTHENIUM OCTAETHYLPORPHYRIN

COMPLEXES WITH SMALL GAS MOLECULES

by

(C) SANDRA GAIL WALKER

B.Sc., The University of Guelph, 1977

A THESIS SUBMITTED IN PARTIAL FULFILMENT OF

THE REQUIREMENTS FOR THE DEGREE OF

MASTER OF SCIENCE

in the department

of

Chemistry

We accept this thesis as conforming

to the required standard

THE UNIVERSITY OF BRITISH COLUMBIA

August, 1980

In presenting this thesis in partial fulfilment of the requirements for an advanced degree at the University of British Columbia, I agree that the Library shall make it freely available for reference and study. I further agree that permission for extensive copying of this thesis for scholarly purposes may be granted by the Head of my Department or by his representatives. It is understood that copying or publication of this thesis for financial gain shall not be allowed without my written permission.
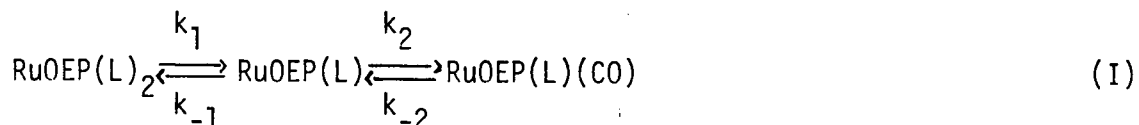
Department of _C HEMISTRY_

The University of British Columbia
2075 Wesbrook Place
Vancouver, Canada
V6T 1W5

Date _17ᵀᴴ SEPT. 1980_

ABSTRACT

Interaction of metalloporphyrins, particularly of the iron subgroup, with gas molecules such as O_2 and CO, remains of considerable interest in terms of comparison with natural heme protein systems. This thesis describes studies on ruthenium(II) porphyrin complexes, the second row analogues of the heme systems.

Toluene solutions of the bis(acetonitrile) complex $RuOEP(CH_3CN)_2$, (OEP = the dianion of octaethylporphyrin) with or without excess acetonitrile present, are irreversibly oxidized by O_2 at $30^{o}C$. However, with CO, the complex undergoes a clean reaction to give $RuOEP(CO)(CH_3CN)$ with several isosbestic points observed in the UV/VIS spectrum. The kinetic dependence on the CO pressure and acetonitrile concentration are consistent with a dissociative mechanism:

$$RuOEP(L)_2 \underset{k_{-1}}{\overset{k_1}{\rightleftharpoons}} RuOEP(L) \underset{k_{-2}}{\overset{k_2}{\rightleftharpoons}} RuOEP(L)(CO) \qquad\qquad (I)$$

The kinetic rate constants, k_1, k_{-2} and k_{-1}/k_2 and the overall equilibrium constant were determined at $30^{o}C$ in toluene.

The $RuOEP(P(n-Bu)_3)_2$ complex, in toluene, is completely unreactive toward O_2 at $30^{o}C$ over a period of several days; although again a monocarbonyl is formed under a CO atmosphere. In the presence of excess $P(n-Bu)_3$, under CO, an equilibrium mixture of $RuOEP(P(n-Bu)_3)_2$ and $RuOEP(CO)(P(n-Bu)_3)$ is formed. The equilibrium constant K for reaction (II) and the thermodynamic parameters ΔH (3.7 Kcal/mole) and ΔS (10.3 e.u.) are determined along with the rate constants for the dissociative mechanism (cf. Equation I). The low ΔH value implies comparable bond

$$RuOEP(P(n-Bu)_3)_2 + CO \underset{K}{\rightleftharpoons} RuOEP(CO)(P(n-Bu)_3) + P(n-Bu)_3 \qquad (II)$$
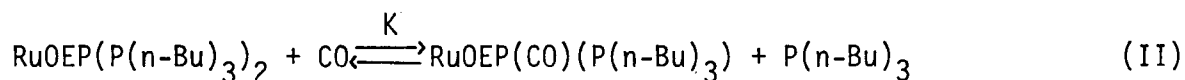
strengths between ruthenium and the two ligands $P(n-Bu)_3$ and CO.

The k_{-1}/k_2 values for the acetonitrile and phosphine systems are thought to relate to the structure of the five-coordinate intermediate, RuOEP(L); the data suggest the ruthenium is probably more in the porphyrin plane than out of plane, al least compared to analogous iron systems. The major difference between the acetonitrile and phosphine systems is in the k_{-2} value which varies by 10^5, partially due to the difference in π-acidity of the two axial ligands.

Toluene solutions of $RuOEP(CH_3CN)_2$ bind N_2 and C_2H_4 very weakly. However, due to the extreme photo- and oxygen-sensitivity of the products, no consistent kinetic data could be obtained.

Solutions of $RuOEP(py)_2$ in neat pyridine, formed in situ from the bis(acetonitrile) complex in pyridine, are completely unreactive toward CO. Even toluene solutions with small amounts of pyridine react only partially ($\sim15\%$ in three days at $25^\circ C$) to give the monocarbonyl.

Upon dissolving the $RuOEP(CH_3CN)_2$ complex in DMA, DMF and THF, the species formed seem to be $RuOEP(CH_3CN)(solvent)$. These species react with CO at $30^\circ C$ in a two step reaction, an instantaneous part followed by a much slower one; the reactions appear to involve the rapid formation of one monocarbonyl followed by decomposition to the expected monocarbonyl, RuOEP(CO)(solvent). Decarbonylation of the amide solvent to give an amine ligand may be involved in the fast reaction.

Judging by the reaction with CO (non-first-order in ruthenium) there

are possibly two species present when $RuOEP(CH_3CN)_2$ is dissolved in pyrrole, $RuOEP(pyrrole)_2$ and $RuOEP(CH_3CN)(pyrrole)$, which react at different rates.

TABLE OF CONTENTS   <ins>Page</ins>

LIST OF TABLES

LIST OF FIGURES

ABBREVIATIONS

The following list of abbreviations, most of which are commonly adopted in chemical research literature, will be employed in this thesis.

atm	atmosphere
A	absorbance at any time, t
A_e	absorbance at the equilibrium position
A_o	absorbance of the reactant
A_t	absorbance at any time, t
A_∞	absorbance of the product
C_2H_4	ethylene
CH_2	methylene
CH_3CN	acetonitrile
^oC	degrees centigrade
cm	centimetre
CO	carbon monoxide
COMb	carbonylated myoglobin
DMA	N,N-dimethylacetamide
DMF	N,N-dimethylformamide
ΔH	enthalpy change for the reaction
^oK	degrees Kelvin
K	equilibrium constant
k_1	kinetic rate constant
k_{-1}	kinetic rate constant
k_2	kinetic rate constant
k_{-2}	kinetic rate constant

k_f	overall rate constant for the forward reaction
k_r	overall rate constant for the reverse reaction
k_{obsd}	pseudo-first-order rate constant
M	molarity
M-CO	metal-carbonyl bond
M(porphyrin)L	five-coordinate metal porphyrin complex
M(porphyrin)L$_2$	six-coordinate metal porphyrin complex
M(porphyrin)L(CO)	carbonylated six-coordinate metal porphyrin complex
M(porphyrin)LL'	mixed axial ligand six-coordinate metal porphyrin complex
mg	milligram
N$_2$	nitrogen
nm	nanometre
O$_2$	dioxygen
OEP	octaethylporphyrin dianion
OMBP	octamethyltetrabenzoporphyrin dianion
Pc	phthalocyanine dianion
P(n-Bu)$_3$	n-butylphosphine
PpIX	protoporphyrin IX
py	pyridine
Ru$_3$(CO)$_{12}$	ruthenium dodecacarbonyl
RuMb	ruthenium(II)-reconstituted myoglobin
RuMb$^+$	ruthenium(III)-reconstituted myoglobin
ΔS	entropy change for the reaction
S	spin state
sec	second
T	temperature

t	time
TCNE	tetracyanoethylene
THF	tetrahydrofuran
TPP	tetraphenylporphyrin dianion
ε	molar extinction coefficient
ν	frequency (cm^{-1})

ACKNOWLEDGEMENTS

CHAPTER I

INTRODUCTION

I.1 General

The interaction of molecular dioxygen (O_2) with metalloporphyrin species has been of interest ever since such species were recognized as being the important centres in naturally occurring oxygen-storage and -transport systems. An iron porphyrin moiety, called a heme unit, is the prosthetic group present in myoglobin and hemoglobin which are involved in oxygen-storage and oxygen-transportation, respectively. Heme units are also components of various oxygenases and oxidases. Oxygenases catalyze the incorporation of one or two atoms of dioxygen into a substrate, while oxidases are enzymes that convert both atoms of dioxygen into water or hydrogen peroxide[1].

These enzyme systems contain proteins which can be difficult to work with, so scientists have been searching for simpler, protein-free co-ordination compounds that can mimic the oxygen-carrying and -activation ability of the natural species. Simple metalloporphyrins seem obvious candidates since, in naturally occurring systems, they are often found at the active site. A study of metalloporphyrin-dioxygen complexes should lead to an increased understanding of the structure and function of certain biological systems employing dioxygen. This subject has been extensively reviewed[1-8], sometimes in context with the more general coverage

of other (non-porphyrin) synthetic oxygen carriers[2-4].

I.2 Hemoglobin and Myoglobin

Hemoglobin and myoglobin combine reversibly with dioxygen and they bind one dioxygen for each heme unit present. The iron atom in the heme unit is chelated to the four core nitrogen atoms of the protoporphyrin IX dianion (Figure I.1).

In the hemeproteins of vertebrates, the porphyrin is embedded in a polypeptide chain having a molecular weight of 16,000 to 18,000. Myoglobins are monomeric, being composed of only one of these protein chains, while most hemoglobins are tetrameric, containing four such polypeptide subunits held together in a tetrahedral array. Each molecule of hemoglobin contains two subunits known as the α chains and two subunits called the β chains. The tertiary structure of the β unit of hemoglobin as deduced from X-ray data is shown in Figure I.2. The protoheme prosthetic group lies in a crevice between E and F helices of the polypeptide, held in place by non-binding interactions with the protein. The single covalent attachment to the protein occurs by coordination of the heme iron to the imidazole nitrogen of the 'proximal' histidine residue[8].

In the deoxygenated state, the ferrous iron is five-coordinate with one vacant axial position. In this conformation, the iron is in a high spin, S=2, configuration and it has been found[9,10] that the metal lies several tenths of an angstrom out of the plane of the porphyrin, towards the axial ligand. Upon oxygenation, the sixth coordination site is occupied by dioxygen and the iron atom now is found in a low spin, S=0, state and moves into the mean plane of the porphyrin[10].

The affinity of a subunit in hemoglobin to add a single molecule of dioxygen is apparently dependent upon the number of other oxygenated

Figure I.1. The stucture of the heme unit of hemoglobin and myoglobin.
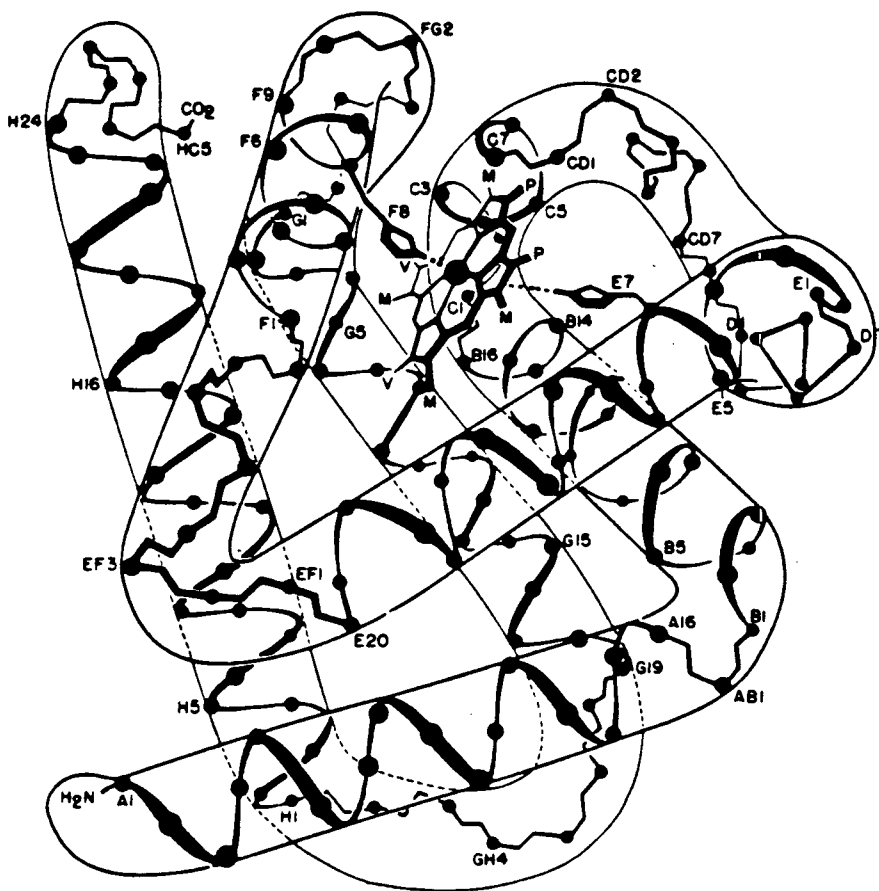
Figure I.2. The structure of the beta chain of hemoglobin. Taken from M. F. Perutz and L. F. TenEyck, Cold Spring Habor Symp. Quant. Biol., 36, 295 (1971).

subunits in the tetramer. This is known as the 'cooperativity effect' and is of great biological importance[10]. The 'Bohr effect' is another important interaction in hemoglobin and relates the change in affinity of the heme site towards the binding of dioxygen as a function of pH[11]. Neither of these effects are present in myoglobin.

I.3 Iron Model Systems

Many porphyrin complexes of transition metals are known to bind dioxygen; these include complexes of cobalt[12], manganese[13], titanium[14] and rhodium[15], but only iron and ruthenium species will be discussed here.

At ambient temperatures, the $Fe(porphyrin)L_2$ (L = any ligand) complexes in a variety of solvents are, in most cases, irreversibly oxidized by dioxygen, often quite rapidly to the final μ-oxo Fe(III) species (Fe(III)-O-Fe(III))[16]. This most likely occurs by a 'dimerization' process involving the interaction of an oxygenated and a deoxy-iron(II) porphyrin[17,18]. These oxo-bridged species are usually five-coordinate and high spin[19]. Another problem in mimicking the protein systems is that ferrous porphyrins tend to form six-coordinate low spin complexes with any ligand present[5], while in deoxymyoglobin, for example, a five-coordiante high spin species is present.

Three recent synthetic approaches[20] based on supressing formation of the μ-oxo diiron complex have led to the formation and detection of 1:1 iron:dioxygen adducts. These methods are 1) use of sterically hindered porphyrins that prevent dimerization, 2) use of low temperatures that slow down the dimerization process, and 3) the use of a rigid surface onto which the iron porphyrin complex can be attached to prevent dimerization. Two other features are desirable to simulate the deoxyheme centre: a five-coordinate geometry and a non-polar hydrophobic environment.

Wang[21] first demonstrated that simple porphyrins could be reversibly oxygenated when immobilized in solid, polymer films. Chang and Traylor[22] then extended this work using solid films of ferrous porphyrins with appended axial ligands, and these systems revealed oxygenation reactions with a 1:1 $Fe:O_2$ stoichiometry. There also were many reports[23] describing reversible, stoichiometric oxygenation of six-coordinate iron(II) porphyrins in solution at low temperatures. Baldwin[24] prepared a capped ferrous porphyrin which reversibly oxygenated in solution at room temperature, as did Collman's more well-known 'picket-fence' porphyrins[25]. These picket-fence porphyrins are synthesized to incorporate a steric bulk on one side of the porphyrin, thereby creating a non-protic cavity for the coordination of ligands such as dioxygen. The geometry protects these complexes from subsequent dimerization reactions. Two such dioxygen adducts have been isolated as solids[25, 26] and are diamagnetic as is oxymyoglobin. The X-ray crystallographic results[27] show that the dioxygen binding is end-on with a bent $Fe-O^O$ bond ($\sim 136°$).

Six-coordinate, low spin $Fe(porphyrin)L_2$ complexes have been shown to react with carbon monoxide at ambient temperatures[28] or with dioxygen at low temperatures[29], to give the carbonyl or dioxygen adduct, respectively, via a dissociative mechanism, equation (1):

$$Fe(porphyrin)L_2 \underset{k_{-1}}{\overset{k_1}{\rightleftharpoons}} Fe(porphyrin)L \underset{k_{-2}}{\overset{k_2}{\rightleftharpoons}} Fe(porphyrin)(L)(X) \qquad (1)$$

$$(X = CO \text{ or } O_2)$$
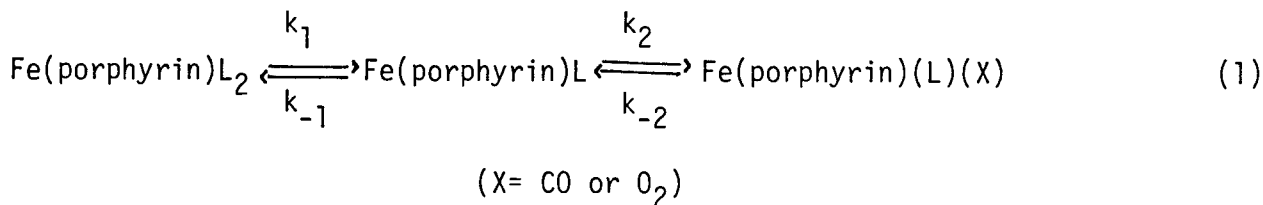
The analysis of the kinetic and equilibrium data yields values of k_1, k_{-2} and k_{-1}/k_2 and these may be compared with data for myoglobin systems. For example, k_{-2} is directly comparable with deoxygenation of oxymyoglobin or

decarbonylation of carbonyl-myoglobin, while the five-coordinate intermediate is considered to be a kinetic model for deoxymyoglobin[28,30]. These data will be discussed in more detail together with data obtained in the present studies on ruthenium systems (Chapters 3 and 4).

I.4 Ruthenium Model Systems

The use of ruthenium instead of iron is a logical extension in both model and protein studies and this has been of prime concern within the Bioinorganic Group here at U.B.C. There seemed, in principle, a good chance of detecting and isolating dioxygen complexes, hopefully under less demanding conditions (see above), since the chemistry of the second row transition metals is generally 'slowed down'.

It was found[31] that solutions of bis(acetonitrile)octaethylporphyrinato-ruthenium(II), $RuOEP(CH_3CN)_2$, (Figure I.3 shows the structure of OEP) in N,N,-dimethylformamide or pyrrole could absorb 1.0 mole of dioxygen per ruthenium atom reversibly at ambient conditions. The system similarly bound carbon monoxide reversibly (cf. equation (1)).

Interestingly, however, ruthenium(II)-reconstituted horse heart apomyoglobin (RuMb) treated with dioxygen in phosphate buffers at 0°C gave only irreversible oxidation to the metmyoglobin, $RuMb^+$, though RuMb did bind CO[32]. Unlike the iron centre, ruthenium is incorporated into myoglobin as a six-coordinate low-spin species and the O_2-oxidation proceeds via an efficient outer sphere mechanism before loss of an axial ligand can occur[29].

It was of interest, then, to study the kinetics of the binding of gas molecules (especially CO and O_2) to the protein-free ruthenium(II) porphyrin complexes for comparison with corresponding iron(II) systems and myoglobin itself.
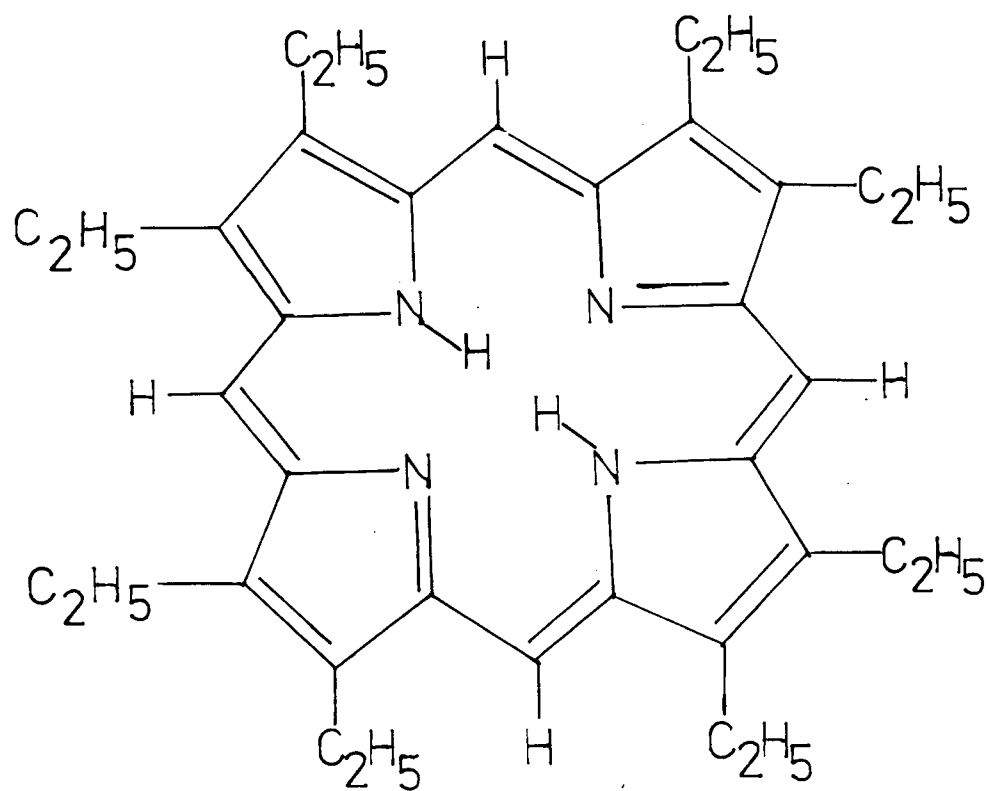
Figure I.3. The structure of octaethylporphyrin.

CHAPTER II

EXPERIMENTAL

II.1 Instrumentation

Ultraviolet and visible absorption spectra were recorded on a Cary 17 spectrophotometer fitted with a thermostated cell compartment. Quartz cells of pathlength 1 cm were used.

Infrared spectra were recorded on a Perkin Elmer 457 grating spectrophotometer. Solid state spectra were obtained as Nujol mulls between NaCl plates.

Nuclear magnetic resonance spectra were recorded on a Varian XL-100 spectrometer.

Microanalyses were performed by Mr. P. Borda of this department.

II.2 Spectrophotometric Kinetic Measurements

Due to the extreme oxygen sensitivity of many of the ruthenium species in solution, it was necessary to perform spectrophotometric studies in a strictly anaerobic system. All optical density measurements in the ultraviolet-visible region were carried out in the type of cell shown in Figure II.1. The cell was maintained at a constant temperature by placing it in a thermostated cell compartment which was attached to a Haake model FK circulating thermostating bath, the temperature of which was adjusted appropriately.

In a typical experiment, the solid ruthenium complex was placed in

the quartz part of the cell through A (Figure II.1) and the solvent was added through B. The solvent was degassed by repeatedly freezing it in the flask of the cell, pumping off any uncondensed gas and then thawing the solvent, being careful not to wet the solid during this process. The degassed solvent could then be added to the solid sample. The cell was then placed in the thermostated compartment to allow the solution temperature to equilibrate. After an initial spectrum was recorded, a known amount of gas was admitted into the cell and the cell was shaken in order to ensure complete mixing of the gas in the solution. The corresponding reaction was then monitored until completion.

Since the concentrations of the ruthenium porphyrin complexes used were very low ($\sim 1 \times 10^{-5}$ M) and the solubilities of the gases are of the order of 1×10^{-3} M atm^{-1}, the gas concentrations in solution and the partial pressure of the gas remained essentially constant throughout the experiment.

The pressure of the gas was measured by a mercury manometer.

II.3 Materials

II.3.1 Gases

Purified argon, nitrogen and oxygen were supplied by Canadian Liquid Air Limited. The argon was further purifed by passing it through a drying tower containing fresh phosphorus pentoxide and molecular sieves (BDH, type 5A). Nitrogen was passed through an 'Oxisorb' catalytic purifier (Alltech Associates) before use.

C.P. Grade carbon monoxide and ethylene were obtained from the Matheson Gas Co. In order to remove any oxygen present from the ethylene, it was frozen in liquid nitrogen and any uncondensed material was pumped off. The frozen gas was then warmed to room temperature and this freeze-pump-warm

A
B

Fitted with a high
vacuum teflon
stopcock

Fitted with B-14 cap

To vacuum line

Quartz cell
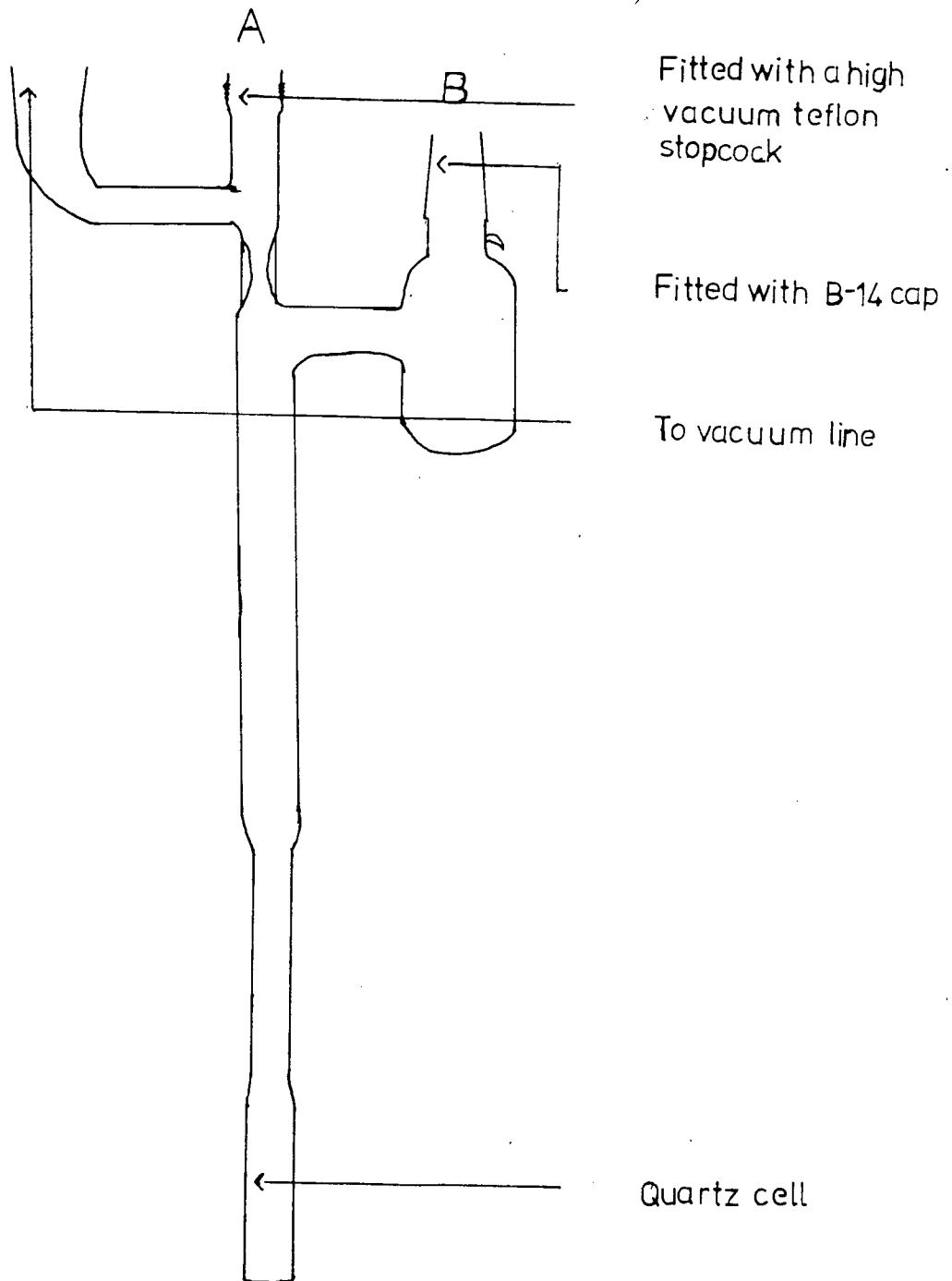
Figure II.1. Anaerobic Spectral Cell.

process was repeated for several cycles until all uncondensed materials were removed.

II.3.2 Solvents

All solvents were freshly distilled prior to use and in all cases, except toluene and acetonitrile, were distilled under vacuum. All solvents, once purified, were handled under an argon atmosphere using Schlenk techniques[33].

Toluene and tetrahydrofuran (Fisher Scientific Co., spectral grade) were dried over and distilled from sodium-benzophenone ketyl, the toluene being distilled under nitrogen. Acetonitrile (Matheson, Coleman and Bell Manufacturing Chemists, spectral grade) was dried over phosphorus pentoxide and distilled from calcium hydride under nitrogen. N,N-Dimethylacetamide (Fisher Scientific Co., analytical grade) and pyrrole (Aldrich Chemical Co. Limited, reagent grade) were dried over and distilled from calcium hydride. N,N-Dimethylformamide (Fisher Scientific Co., analytical grade) was dried over and distilled from anhydrous copper sulphate. Pyridine (American Chemical and Scientific Co., reagent grade) was dried over and distilled from potassium hydroxide.

II.3.3 Nongaseous Ligands

Tri(n-butyl)phosphine (Aldrich Chemical Co. Limited, analytical grade) was vacuum distilled. Tetracyanoethylene (Eastman Kodak Co.) was purified by sublimation.

II.4 Complexes

Carbonyloctaethylporphyrinatoruthenium(II)·ethanol (RuOEP(CO)(EtOH)) was prepared by a method similar to that of Tsutsui et al[34]. 500 mg of octaethylporphyrin, provided by J. B. Paine III, and 500 mg of Ru_3CO_{12}

(Strem Chemical Inc.) were refluxed in 100 ml of degassed toluene, under N_2, for 24 hours. The toluene was removed and the solid dissolved in 25 ml of methylene chloride and 25 ml of absolute ethanol. This solution was refluxed under N_2 for thirty minutes before the solvent was removed and the solid was purified by chromatography. A deactivated alumina (Fisher Scientific Company, 80-200 mesh) column was made up in petroleum ether (reagent grade, 65°-110°C) and the product was eluted using petroleum ether, toluene and ethanol. The complex was recrystallized from methylene chloride/ethanol, washed with pentane and dried (64% yield); $\nu_{CO}=1930$ cm^{-1}.

Analysis: Calculated for $C_{39}H_5N_4O_2Ru$: C, 66.19%; H, 7.07%; N, 7.92%. Found: C, 66.11%; H, 7.15%; N, 7.92%.

Nuclear Magnetic Resonance data in CDCl$_3$: OEP; CH$_3$, 1.98 triplet; CH$_2$, 4.09 quartet; pyrrole, 9.98 singlet; Ethanol; CH$_2$, -1.06 triplet; CH$_3$, -0.07 quartet.

Bis(acetonitrile)octaethylporphyrinatoruthenium(II) (RuOEP(CH$_3$CN)$_2$) was prepared based on a general photolysis method described by Whitten et al[35]. 200 mg of RuOEP(CO)(EtOH) was dissolved in 100 ml each of degassed acetonitrile and toluene under argon in a photolysis cell (Figure II.2). Argon was bubbled through the stirring solution as it was irradiated for 18 hours with a Hanovia medium pressure 450-W mercury vapour bulb. The solvent was then removed on a vacuum line and the solid was washed with cold pentane and dried (72% yield); $\nu_{C\equiv N}=2260$ cm^{-1} [31].

Analysis: Calculated for $C_{40}H_{50}N_6Ru$: C, 67.13%; H, 6.99%; N, 11.75%. Found: C, 67.41%; H, 6.96%; N, 11.25%.

Nuclear Magnetic Resonance data in CDCl$_3$: OEP; CH$_3$, 1.90 triplet; CH$_2$, 4.00 quartet; pyrrole, 9.90 singlet; Acetonitrile; CH$_3$, 0.64 singlet.
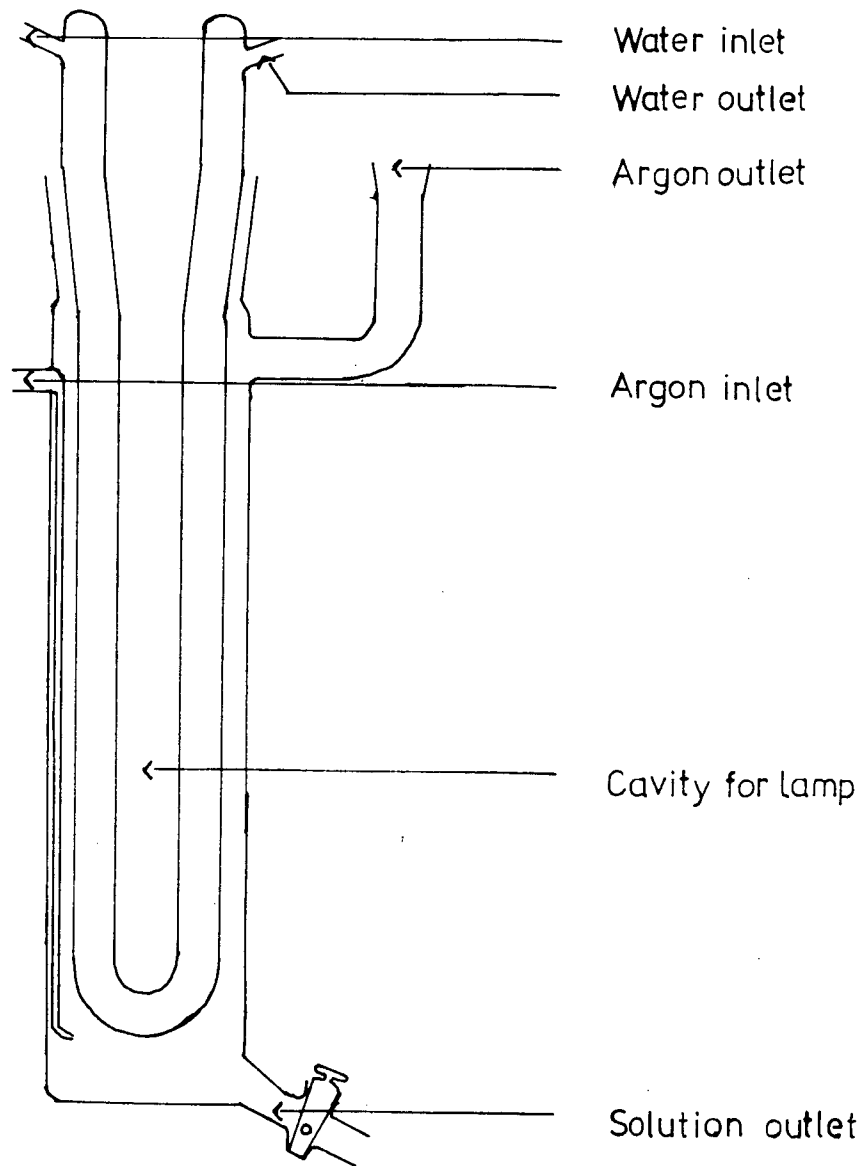
Figure II.2. Photolysis Cell.

Bis(tri(n-butyl)phosphine)octaethylporphyrinatoruthenium(II) (RuOEP(P(n-Bu)$_3$)$_2$) was generously provided by Dr. George Domazetis.

Dilute solutions of RuOEP(L)$_2$ species (L = solvent) can be made in situ. Solutions of 10^{-5} M RuOEP(CO)(EtOH) are made up in the spectral cell in the appropriate solvent. The solution is then irradiated with a 600 W B1-PIN tungsten halogen lamp until the spectrum observed is that of the RuOEP(L)$_2$ species (∿2 min). The solution can then be degassed to remove some of the CO released during the photolysis.

CHAPTER 3

THE REACTION OF RuOEP(CH$_3$CN)$_2$ AND CO

III.1 Spectral Characteristics

Toluene was chosen as a solvent to study the reactions of O$_2$ and CO with the RuOEP(CH$_3$CN)$_2$ complex. However, when the initial spectrum of the bisacetonitrile complex was recorded, under argon in dilute solution ($\sim 10^{-5}$ M), the visible bands were very broad and not typical of six-coordinate, low spin Ru(II)[36]. Since acetonitrile, as an axial ligand, may be quite labile, and not strongly coordinated, acetonitrile was added to the toluene solution in order to generate and stabilize the six-coordinate species in solution and achieve the corresponding spectrum.

Toluene solutions of RuOEP(CH$_3$CN)$_2$ under an atmosphere of O$_2$ slowly undergo irreversible oxidation; the product is likely a μ-oxo Ru(III) dimer as is usually observed with the corresponding six-coordinate protein-free iron porphyrin systems.

The RuOEP(CH$_3$CN)$_2$ species under an atmosphere of CO underwent a series of spectral changes to give a final spectrum identical to that of RuOEP(CO)(CH$_3$CN) (made by dissolving $\sim$5 x 10^{-5} M RuOEP(CO)(EtOH) in a 10^{-3} M solution of acetonitrile in toluene). Measurements of CO uptake by the RuOEP(CH$_3$CN)$_2$ species showed that 1.0 mole of CO/Ru atom was absorbed[31].

Figure III.1 shows typical spectral changes, as a function of time, for the addition of a known amount of CO to RuOEP(CH$_3$CN)$_2$; a number of
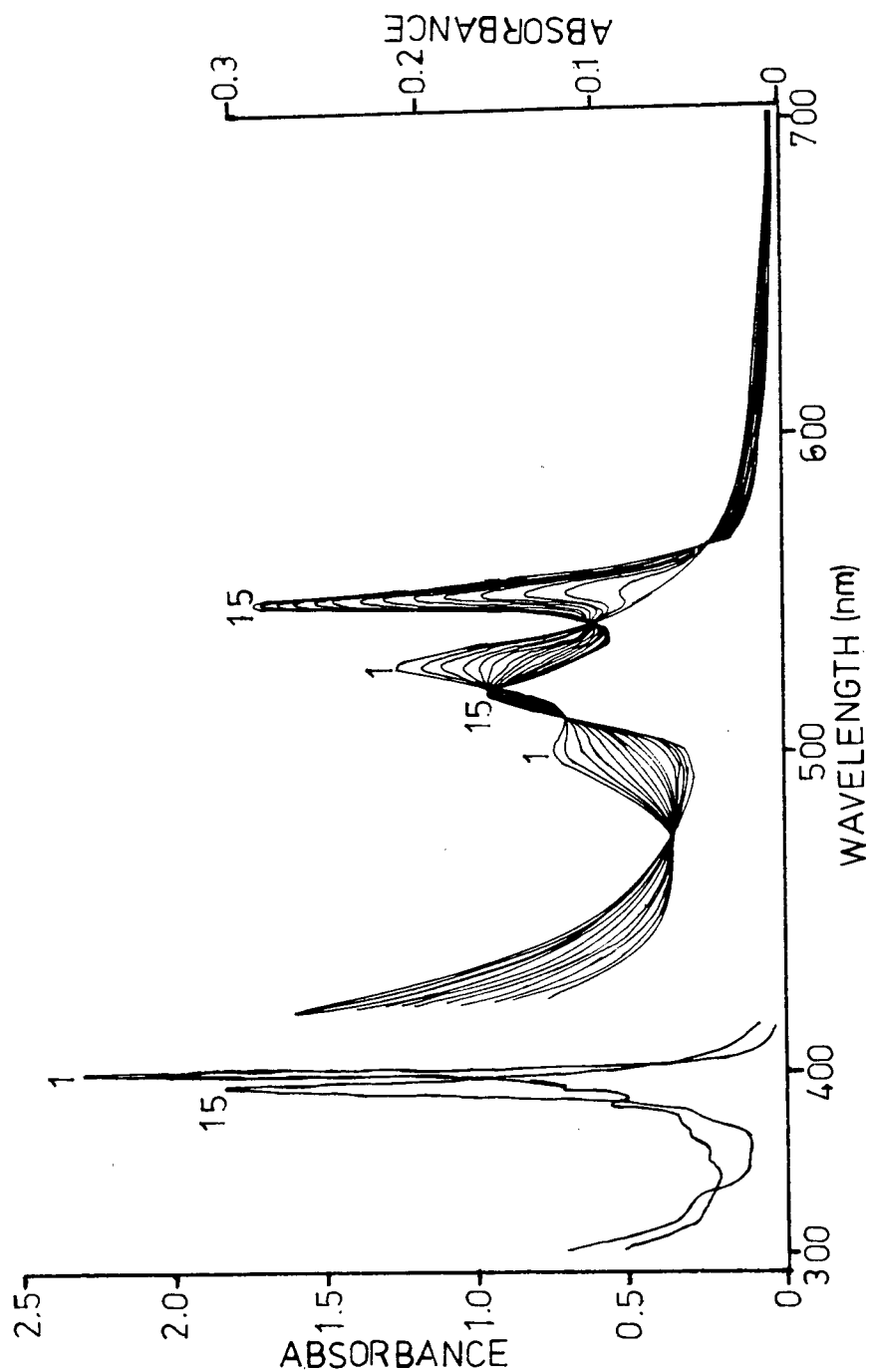
Figure III.I. Typical Spectral Changes for the Reaction of RuOEP(CH$_3$CN)$_2$ with CO in Toluene at 30°C.

isosbestic points are generated. In the visible region, the bands at 527 nm (ϵ = 1.70 x 10^4 M^{-1} cm^{-1}) and 496 nm (ϵ = 1.05 x 10^4 M^{-1} cm^{-1}) red shift to positions at 549 nm (ϵ = 2.29 x 10^4 M^{-1} cm^{-1}) and 518 nm (ϵ = 1.31 x 10^4 M^{-1} cm^{-1}). The Soret region with an intense band at 405 nm (ϵ = 2.20 x 10^5 M^{-1} cm^{-1}) and smaller side bands at 394 nm (ϵ = 8.46 x 10^4 M^{-1} cm^{-1}) and 385 nm (ϵ = 6.93 x 10^4 M^{-1} cm^{-1}) changed to a major band at 395 nm (ϵ = 1.76 x 10^5 M^{-1} cm^{-1}) with a small shoulder at 375 nm. For a fixed CO pressure, the length of time required for each reaction increased with increasing added concentration of acetonitrile in the solution.

III.2 Treatment of Data

The kinetic data were obtained by following the increase in spectral intensity of the 549 nm band of the carbonyl. Plots of $\log(A_\infty - A_t)$ versus time gave good straight lines, Figure III.2;

A_∞ is the absorbance of the RuOEP(CO)(CH$_3$CN) species

and A_t is the absorbance at any time, t, during the reaction.

This shows that the reaction follows pseudo-first-order kinetics under the conditions of the experiment. The CO concentration is much larger than that of the porphyrin(see below). An inverse dependence on acetonitrile concentration at a fixed CO pressure and a less than first-order dependence on CO at a fixed acetonitrile concentration are readily interpreted in terms of a dissociative mechanism(Eq. 1, Ch. 1):

$$\text{RuOEP(CH}_3\text{CN)}_2 \underset{k_{-1}}{\overset{k_1}{\rightleftharpoons}} \text{RuOEP(CH}_3\text{CN)} \underset{k_{-2}}{\overset{k_2}{\rightleftharpoons}} \text{RuOEP (CO)(CH}_3\text{CN)} \qquad (2)$$
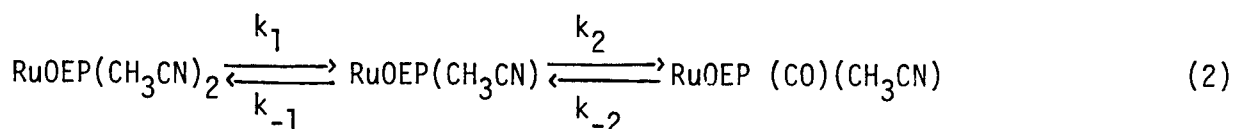
Since the reaction is judged, by the spectral changes, to go to completion, k_{-2} is assumed to be negligible. Assuming a steady state
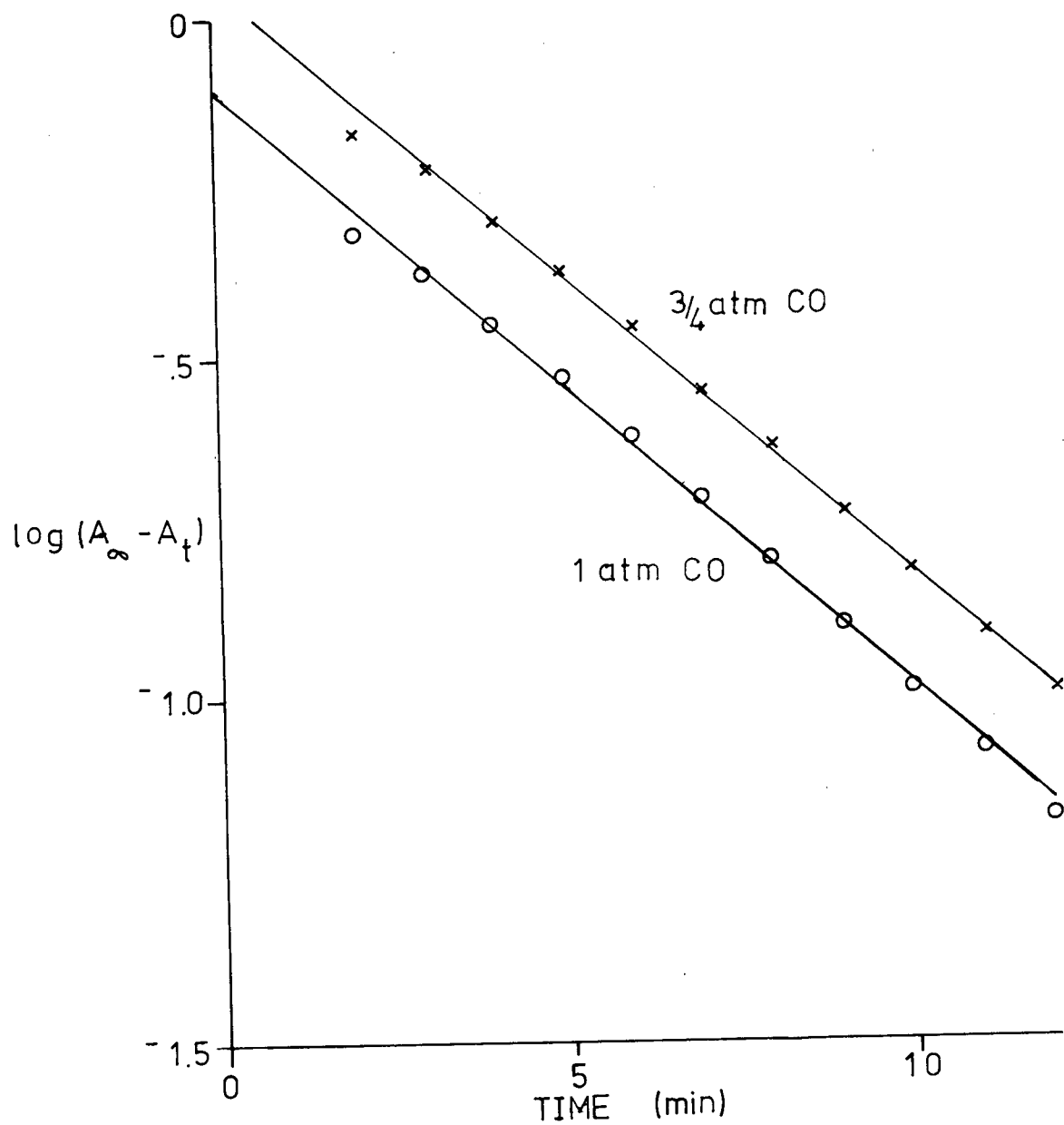
Figure III.2. First-Order Plots for the Reaction of $RuOEP(CH_3CN)_2$ With CO in Toluene With 1.91×10^{-2} M Acetonitrile added at $30^{\circ}C$.

concentration of five-coordinate intermediate leads to the rate law:

$$\text{rate} = \frac{k_1 k_2 [CO] [RuOEP(CH_3CN)_2]}{k_{-1} [CH_3CN] + k_2 [CO]} \tag{3}$$

For any one experiment in which the CO and acetonitrile concentrations remain effectively constant, this may be rewritten as:

$$\text{rate} = k_{obsd} [RuOEP(CH_3CN)_2]$$

where $k_{obsd} = k_1 k_2 [CO]/(k_{-1} [CH_3CN] + k_2 [CO])$ (4)

k_{obsd} is the pseudo-first-order rate constant measured in the plots of $\log(A_\infty - A_t)$ versus time.

The data are given in Table III.1. In agreement with equation (4), at high acetonitrile concentrations, the dependence on CO pressure approaches first-order but becomes less than first-order and approaches zero order as the acetonitrile concentration decreases. The acetonitrile dependence remains inverse over the small pressure range of CO studied. There were no complications in the system due to the presence of displaced acetonitrile in the forward reaction since added acetonitrile was at least in a hundred-fold excess.

The inverse of expression (4) gives:

$$k_{obsd}^{-1} = k_1^{-1} + k_{-1} [CH_3CN]/(k_1 k_2 [CO]) \tag{5}$$

The CO pressure can be converted to molarity using the known solubility of CO in toluene at $30^\circ C$ (6.5×10^{-3} M atm^{-1})[37]. A plot of k_{obsd}^{-1} vs $[CH_3CN]/[CO]$ for all data in Table III.1 gives a straight line of slope $k_{-1}/k_1 k_2$ and an intercept of k_1^{-1} (e.g. Figure III.3). The value of k_{-2} was estimated by placing the solid RuOEP(CO)(EtOH) adduct into a large excess of acetonitrile in toluene solution and following spectral changes for the CO displacement by acetonitrile. The overall equilibrium constant K

Table III.1. <u>Rate of Reaction of RuOEP(CH$_3$CN)$_2$ With CO in Toluene at</u>

<u>Various Acetonitrile Concentrations and CO Pressures, at 30°C.</u>

CO Pressure[a] (atm)	[CH$_3$CN] (moles/litre)	$k_{obsd} \times 10^4$ [b] (sec^{-1})
0.963	0.375	1.95
0.963	0.190	3.70
0.713	0.190	2.77
0.463	0.190	1.97
0.213	0.190	1.18
0.971	9.52×10^{-2}	6.47
0.721	9.52×10^{-2}	4.37
0.501	9.52×10^{-2}	3.08
0.221	9.52×10^{-2}	2.12
0.971	5.72×10^{-2}	9.33
0.721	5.72×10^{-2}	6.97
0.471	5.72×10^{-2}	5.63
0.241	5.72×10^{-2}	3.48
0.971	3.82×10^{-2}	10.53
0.721	3.82×10^{-2}	9.12
0.471	3.82×10^{-2}	7.47
0.221	3.82×10^{-2}	4.35
0.971	1.91×10^{-2}	15.72
0.721	1.91×10^{-2}	14.58
0.471	1.91×10^{-2}	11.57
0.221	1.91×10^{-2}	7.00
0.971	3.83×10^{-3}	23.98
0.721	3.83×10^{-3}	21.92
0.471	3.83×10^{-3}	20.03
0.221	3.83×10^{-3}	16.67

a. Pressures were corrected for the partial pressure of toluene at 30°C; R. C. Weast, Ed., 'Handbook of Chemistry and Physics', 56th standard ed., The Chemical Rubber Company Co., Cleveland, Ohio, 1975, p D198.

b. estimated error ±5%.
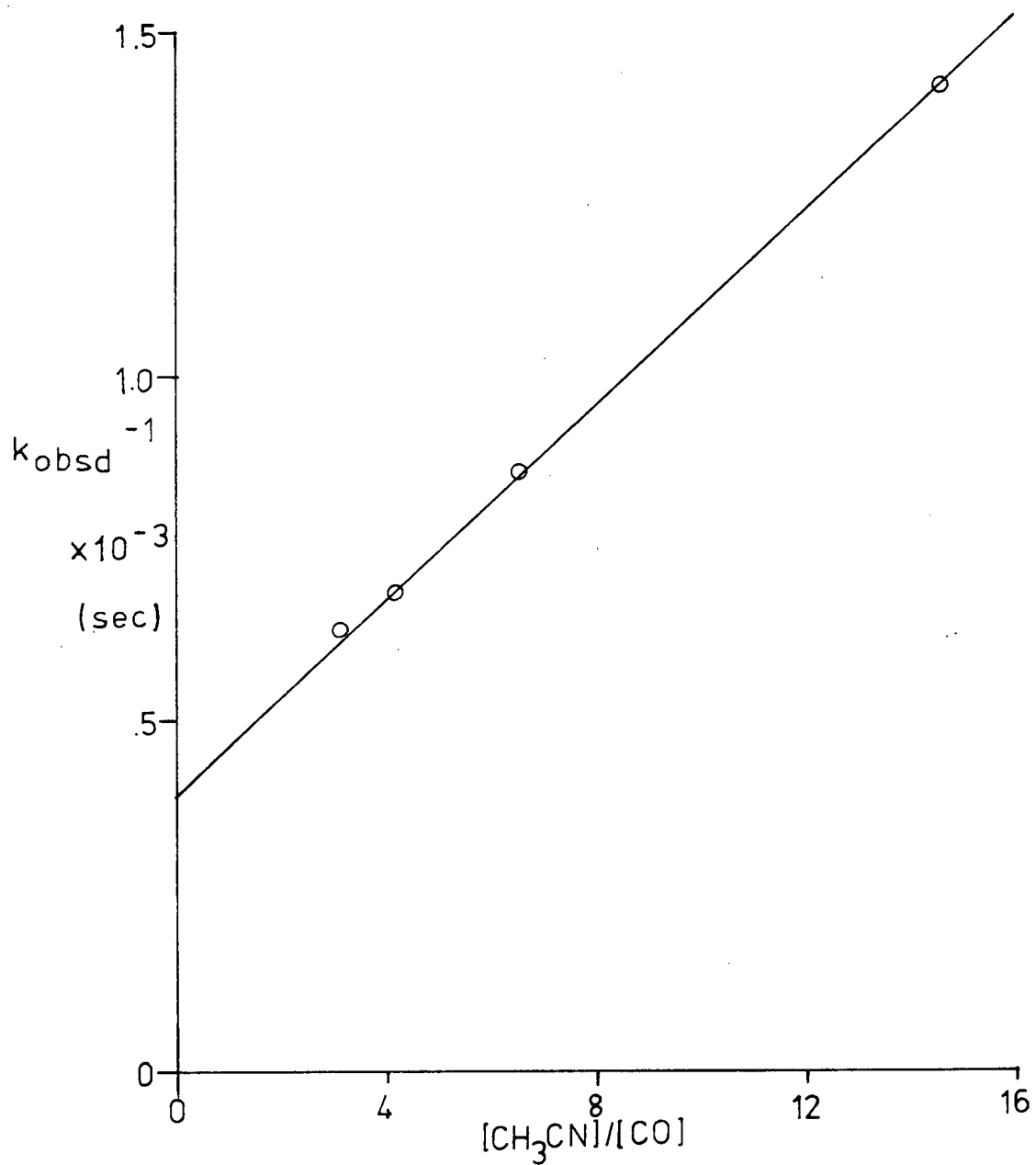
Figure III.3. Plot of k_{obsd}^{-1} vs $[CH_3CN]/[CO]$ For The Reaction of RuOEP(CH_3CN)_2 With CO in Toluene With 1.91×10^{-2} M Acetonitrile Added at 30^{0}C.

$(k_1k_2/k_{-1}k_{-2})$ can then be readily estimated (see below).

Table III.2. <u>Kinetic and Equilibrium Data for the Reaction of RuOEP(CH$_3$CN)$_2$ With CO at 30°C in Toluene.</u>

k_1 [a] (sec^{-1})	k_{-1}/k_2 [b]	k_{-2} (sec^{-1})	K
2.41×10^{-3}	.176	3.4×10^{-7}	4.0×10^4

a. estimated error ±25%.   b. estimated error ±10%.

III.3 <u>Discussion</u>

From the data, the six-coordinate bis(acetonitrile) complex is seen to lose an acetonitrile ligand about 10^4 times faster than the mixed ligand species gives up a CO molecule and this is the major factor governing the equilibrium constant. The k_{-1}/k_2 value shows that the five-coordinate intermediate prefers to bind CO over acetonitrile kinetically by a factor of about five.

Some rough calculations based on unpublished data from these laboratories[38], were done[39] (Table III.3) for oxygen binding of RuOEP(pyrrole)$_2$ in pyrrole, which is a solvent in which oxygenation occurs without appreciable oxidation. The values for k_1 and k_{-1}/k_2 are comparable to the CO reaction in toluene but there is a difference of about a hundred in k_{-2} and the values suggest that the strong binding of CO (compared to O$_2$) is reflected in its much lower off-rate. Attempts to measure the kinetics of the CO reaction with RuOEP(CH$_3$CN)$_2$ in pyrrole for a more direct comparison with the O$_2$ system were unsuccessful (see Chapter 5).

Table III.3. <u>Kinetic and Equilibrium Data for the Reaction of RuOEP(pyrrole)$_2$</u>

<u>With O$_2$ at 20°C in Pyrrole.</u>

k_1 (sec^{-1})	k_{-1}/k_2	k_{-2} (sec^{-1})	K
~0.003	~0.06	~10^{-5}	~10^4

It is also of interest to compare the RuOEP(CH$_3$CN)$_2$/CO data with those for the CO binding to some Fe(porphyrin)(amine)$_2$ systems[28-30] (Table III.4). In terms of porphyrin properties, OEP is considered much closer to protoporphyrin IX (PpIX) than octamethyltetrabenzoporphyrin (OMBP) or tetraphenylporphyrin (TPP) or phthalocyanine (Pc).

Table III.4. <u>Kinetic and Equilibrium Data[30] for the Reaction of</u>

<u>Fe(porphyrin)(piperidine)$_2$ Complexes With CO in Toluene</u>

<u>at 23°C.</u>

Porphyrin	k_1 (sec^{-1})	k_{-2} (sec^{-1})	k_{-1}/k_2	K
OMBP	1020	0.25	1.7	2340
	490[a]	0.09[a]	26[a]	209[a]
PpIX	20	0.06	0.002	230000
TPP	11	0.52	0.002	150000
Pc	0.5	0.13	3.3	0.85

a. Fe(OMBP)(py)$_2$

The k_{-1}/k_2 value for $RuOEP(CH_3CN)_2$ in toluene lies within the range

of data for the iron systems and is some 100 times the value for the PpIX

system. The k_1 and k_{-2} values are quite different for the ruthenium and

iron systems. The k_1 value for the FePpIX system is some 10^3 times that

of the ruthenium complex and 10^5 times the k_{-2} value. As expected, kinetic

lability is slowed down considerably when using the second row elements.

The k_{-2} value for $RuOEP(CH_3CN)_2/CO$ can also be compared to the

decarbonylation rate of COMb in aqueous solution at pH 7, $20^\circ C^{39}$ $(k_{-2}$

~ 0.02 $sec^{-1})$. Although the k_{-2} value for COMb is similar to the k_{-2}

values of the iron protein-free systems, once again the ruthenium complex

binds CO much tighter kinetically than the naturally occurring heme group does.

Based on the findings in the iron systems (Table III.4), a hypothesis

was advanced dealing with the geometry of the five-coordinate intermediate[40],

and such consideration should also be extended to the ruthenium systems.

The two possible extreme structures for the five-coordinate intermediate

are shown in Figure III.4.
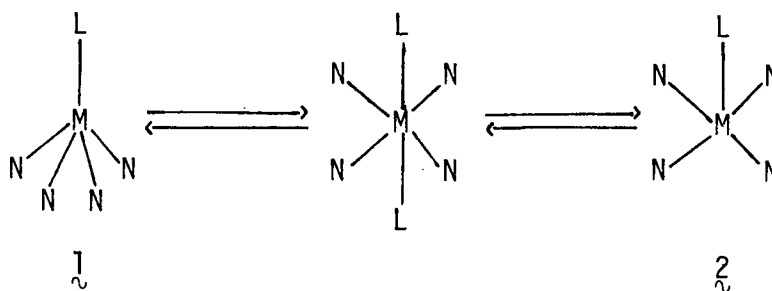
Figure III.4 Possible Structures of the Five-Coordinate Intermediate.

When considering steric interactions, the addition of a bulky ligand

to a high spin intermediate, 1, will be less favourable than the corresponding

addition to the low spin species, $\underset{\sim}{2}$, especially relative to the rate of addition of a non-bulky ligand such as CO.

If the assumption is made that the intermediate lies close to the transition state, both in free energy and geometry[41], then some statement about the structure of the intermediate can be made, based on the kinetic data. In Table III.4, there is a range of 10^3 for the k_{-1}/k_2 values and this variation may arise from a difference in structure and spin state of the intermediate. The five-coordinate intermediate of the PpIX and TPP systems was considered to have a structure similar to that of $\underset{\sim}{1}$ which resembles the active site of hemoglobin and myoglobin, with the iron atom out of the plane and in a high spin state. The larger values of k_{-1}/k_2 for OMBP and Pc would be consistent with an intermediate species that is low or intermediate spin with a structure closer to that of $\underset{\sim}{2}$.

The k_{-1}/k_2 value of 0.176 for the ruthenium system might imply a structure more analagous to $\underset{\sim}{2}$ than $\underset{\sim}{1}$ for the RuOEP(CH$_3$CN) intermediate, but clearly much more data are needed for other ruthenium systems (especially with Ru(porphyrin)(amine)$_2$ species) before such a conclusion can be drawn. An axial piperidine ligand in an iron porphyrin system does give rise to steric interaction due to the 2,6-CH$_2$ groups[42] and thus could well give rise to movement of the iron atom out of the plane in the five-coordinate intermediate. The k_{-1}/k_2 value for the FePpIX(py)$_2$/CO system with no such steric problem is likely to be greater than the 0.002 value for the piperidine system. Using the OMBP data as a guide, (Table III.4), the k_{-1}/k_2 value could be increased to $\sim$0.02, a factor of about ten smaller than the ruthenium system: the data again tentatively suggest a more in-plane structure for the ruthenium intermediate.

CHAPTER 4

THE REACTION OF RuOEP(P(n-Bu)$_3$)$_2$ AND CO

IV.1 Spectral Characteristics

Toluene was again used as the solvent for this system. However, it was not necessary to add an excess of phosphine ligand to the solvent in order to generate the correct spectrum for the six-coordinate bis(phosphine) system. This contrasts with the bis(acetonitrile) system in toluene (Chapter 3).

When one atmosphere of O$_2$ was added to the bis(phosphine) system at 30°C, no appreciable reaction occurred within 24 hours. Upon addition of one atmosphere of CO, however, a series of spectral changes were observed as a function of time. There were several clean isosbestic points and the reaction appeared to go to completion to form the carbonyl-phosphine complex. To establish pseudo-first-order conditions with respect to ligand concentration, small amounts of phosphine were added to the toluene in all reactions. However, under these conditions, the reaction did not go to completion, the position of the equilibrium being dependent upon the CO pressure used and the amount of excess phosphine added.

Figures IV.1 and IV.2 show typical spectral changes characteristic of the reaction. The product, RuOEP(P(n-Bu)$_3$)(CO), was never isolated so its extinction coefficients were based on the spectrum achieved when the reaction went to completion with no added phosphine ligand.
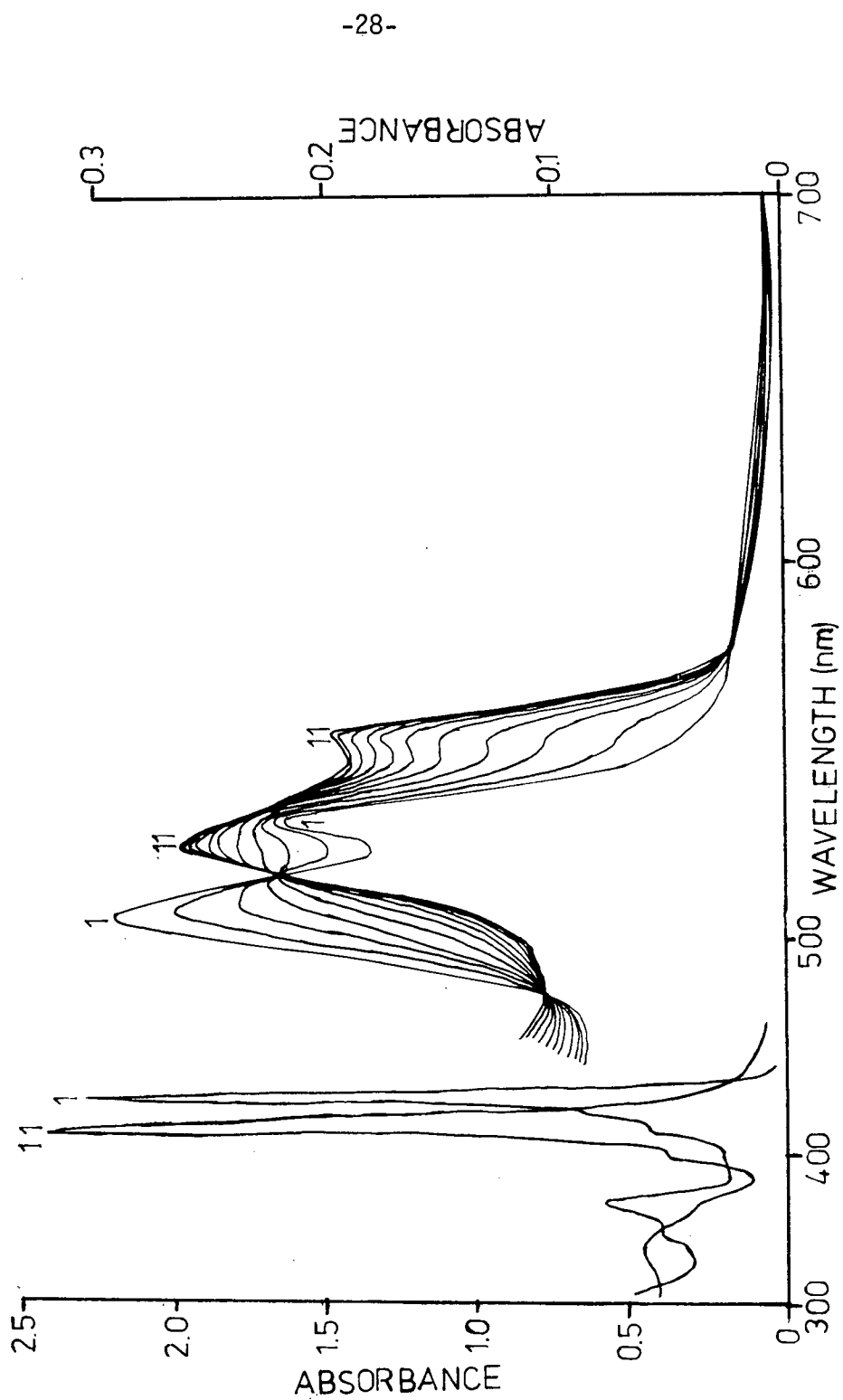
Figure IV.1. Spectral Changes for the Reaction of RuOEP(P(n-Bu)$_3$)$_2$ with 1 atm CO in Toluene with no added P(n-Bu)$_3$ at 31°C.
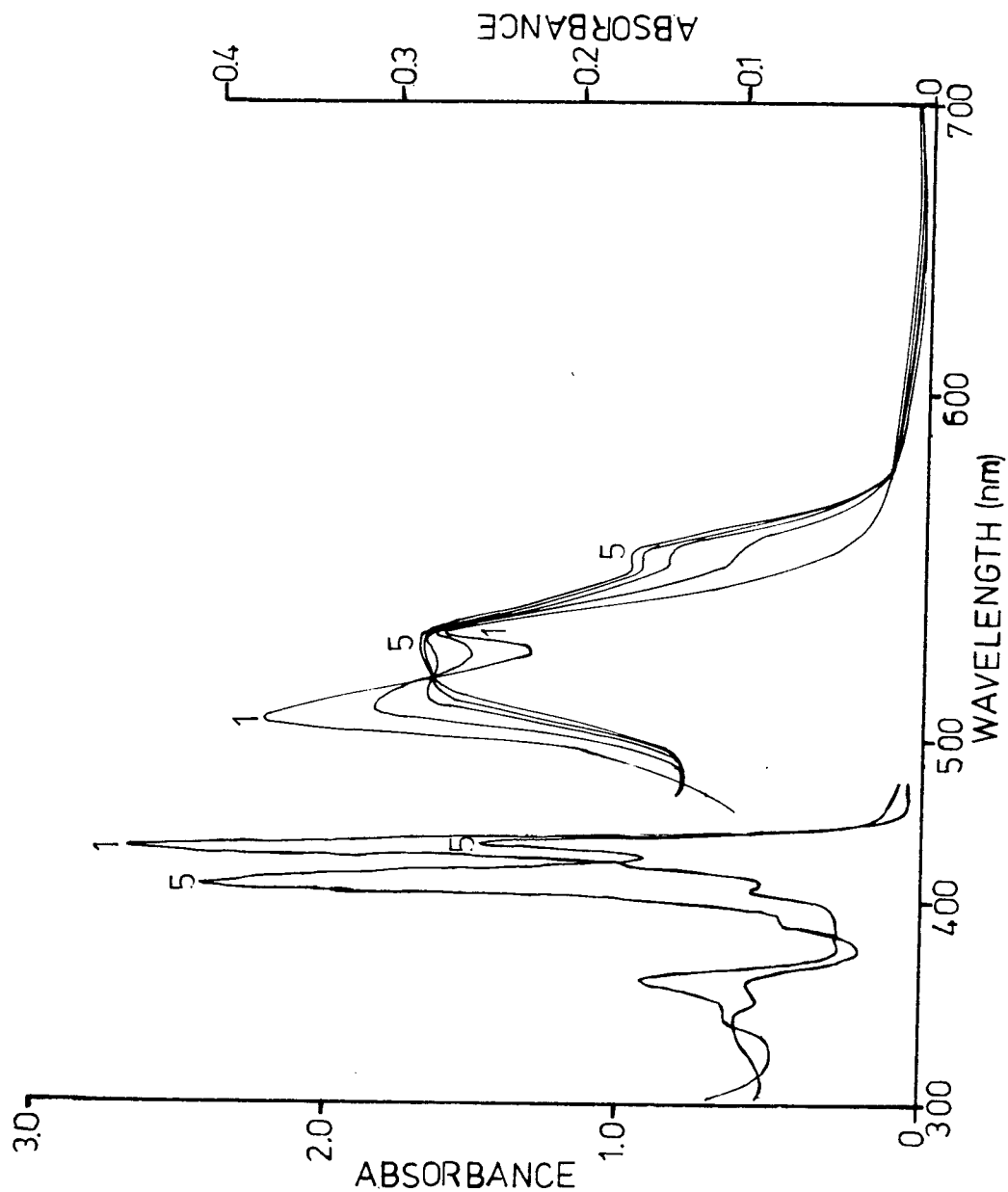
Figure IV.2. Spectral Changes for the Reaction of $RuOEP(P(n-Bu)_3)_2$ with 1 atm CO in Toluene Containing 2.84×10^{-4} M $P(n-Bu)_3$ at $31^\circ C$.

In the initial spectrum of $RuOEP(P(n-Bu)_3)_2$, there are bands at 535 nm (ε = 1.95 x 10^4 M^{-1} cm^{-1}), 511 nm (ε = 2.72 x 10^4 M^{-1} cm^{-1}), ∿460 nm (ε = 0.51 x 10^4 M^{-1} cm^{-1}), 428 nm (ε = 3.20 x 10^5 M^{-1} cm^{-1}), 417 nm (ε = 7.98 x 10^4 M^{-1} cm^{-1}), 405 nm (ε = 4.94 x 10^4 M^{-1} cm^{-1}), 360 nm (ε = 7.72 x 10^4 M^{-1} cm^{-1}) and ∿341 nm (ε = 5.06 x 10^4 M^{-1} cm^{-1}). The final spectrum of $RuOEP(P(n-Bu)_3)(CO)$ has bands at 555 nm (ε = 1.70 x 10^4 M^{-1} cm^{-1}), 528 nm(ε = 2.39 x 10^4 M^{-1} cm^{-1}), 409 nm (ε = 3.49 x 10^5 M^{-1} cm^{-1}), 388 nm (ε = 6.74 x 10^4 M^{-1} cm^{-1}), 358 nm (ε = 5.84 x 10^4 M^{-1} cm^{-1}) and ∿325 nm (ε = 7.62 x 10^4 M^{-1} cm^{-1}). At any particular equilibrium position, there were bands of both the starting and final species (cf. Figure IV.2). In most cases, reactions were over within twenty minutes.

IV.2 Treatment of Data

The dependence of the reaction on CO pressure and the concentration of added phosphine is consistent with the equilibrium:

$$RuOEP(P(n-Bu)_3)_2 + CO \overset{K}{\rightleftharpoons} RuOEP(P(n-Bu)_3)(CO) + P(n-Bu)_3 \qquad (6)$$
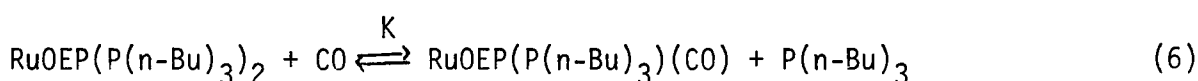
$$K = \frac{[RuOEP(P(n-Bu)_3)(CO)]\,[P(n-Bu)_3]}{[RuOEP(P(n-Bu)_3)_2]\,[CO]} \qquad (7)$$

Using spectral data to find the various concentrations of initial and final species, one can rewrite the equilibrium expression as:

$$\log K = \log \frac{A_0-A}{A-A_\infty} - \log[CO] + \log[P(n-Bu)_3] \qquad (8)$$

A_0 is the absorbance of the RuOEP(P(n-Bu)$_3$)$_2$ species

A_∞ is the absorbance of the RuOEP(P(n-Bu)$_3$)(CO) species estimated by extinction coefficient data

A is the absorbance at the equilibrium position.

The CO pressure is again converted to molarity units[36].

Temperature dependence studies were done over a range of 21-41°C. The equilibrium constants were obtained from plots of log $\frac{A_0-A}{A-A_\infty}$ vs

log [P(n-Bu)$_3$] at a fixed pressure (Figure IV.3). In all cases, straight line plots of slope -1.0 ± .1 were obtained. The K values are listed in Table IV.1. A plot of ln(K) vs 1/T (Figure IV.4) gave a straight line from which the thermodynamic parameters, ΔH = 3.7 ± 0.5 Kcal/mole and ΔS = 10.3 ± 5 e.u., were calculated.

Table IV.1 <u>Equilibrium Constant Values from 21-41°C for the Reaction</u>
<u>of RuOEP(P(n-Bu)$_3$)$_2$ with one Atmosphere CO, in Toluene.</u>

Temperature (°C)	21	26	31	36	41
K[a]	0.425	0.506	0.536	0.589	0.650

a. estimated error ± 10%.

As well as calculating a value for K and its thermodynamic parameters, some individual kinetic rate constants were also determined. Kinetic data were obtained by following the increase in spectral intensity at 555 nm as CO was bound by the ruthenium. In these cases, though, since the reactions did not go to completion, the rate law expression used in Chapter 3 cannot be used.

The dissociative mechanism is once more assumed to be occurring, i.e.
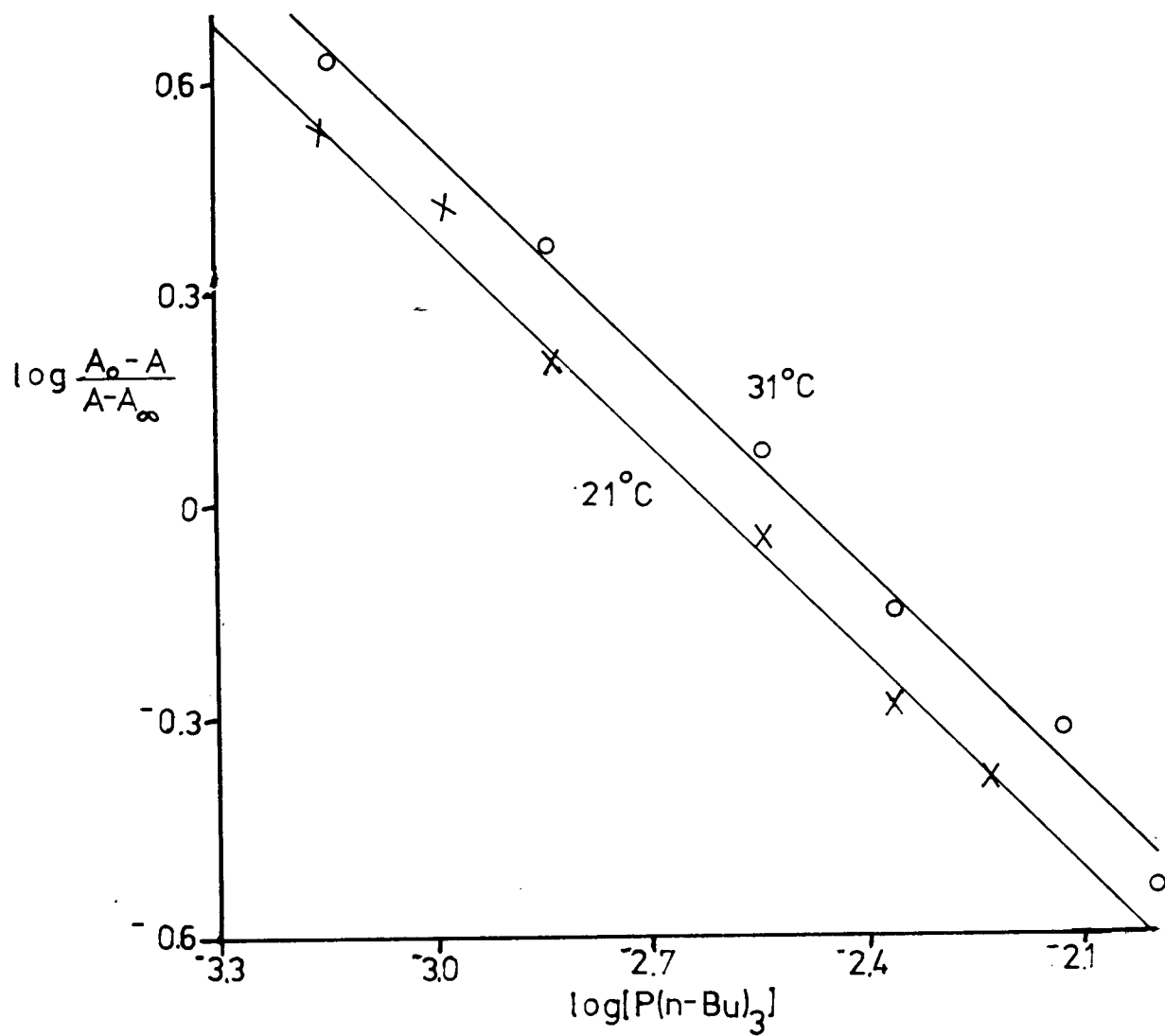
Figure IV.3. Equilibrium Plots for the Reaction of $RuOEP(P(n-Bu)_3)_2$ with 1 atm CO in Toluene.
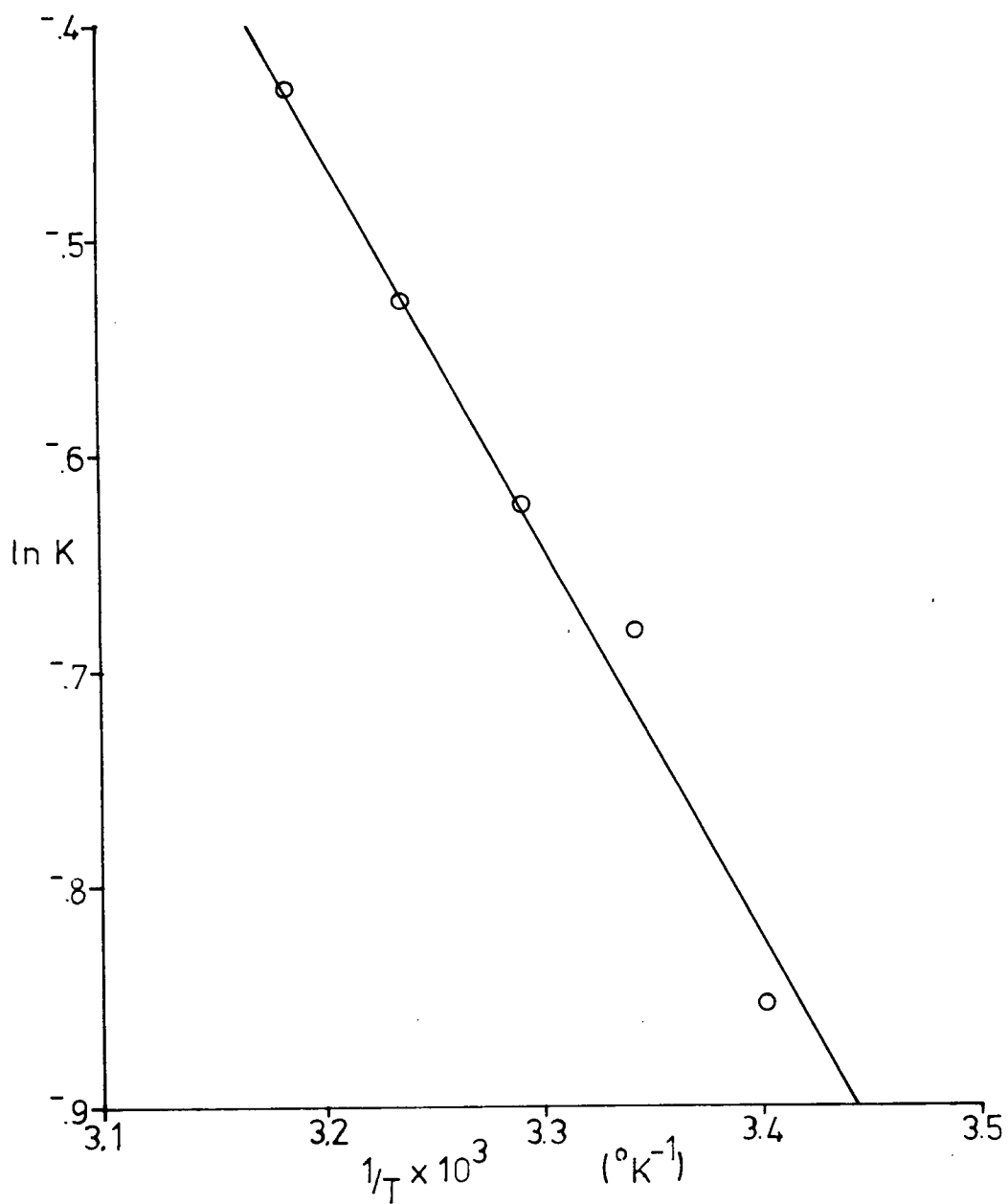
Figure IV.4. Van't Hoff Plot for the Reaction of RuOEP(P(n-Bu)$_3$)$_2$ with 1 atm CO in Toluene.

$$\text{RuOEP(P(n-Bu)}_3)_2 \underset{k_{-1}}{\overset{k_1}{\rightleftharpoons}} \text{RuOEP(P(n-Bu)}_3) \underset{k_{-2}}{\overset{k_2}{\rightleftharpoons}} \text{RuOEP(P(n-Bu)}_3)(\text{CO}) \qquad (9)$$
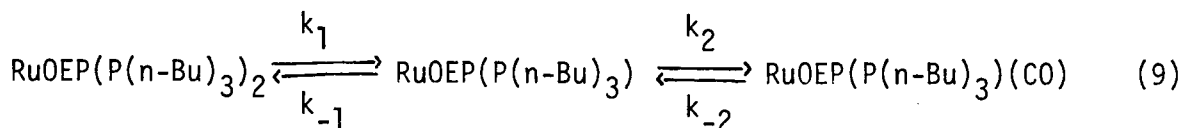
but since an equilibrium is obtained in all cases, k_{-2} cannot be assumed negligible. Therefore, when the rate law is derived, the expression becomes:

$$\text{rate} = \frac{k_1 k_2 [\text{CO}] [\text{RuOEP(P(n-Bu)}_3)_2]}{k_{-1}[\text{P(n-Bu)}_3] + k_2[\text{CO}]} - \frac{k_{-1}k_{-2}[\text{P(n-Bu)}_3][\text{RuOEP(P(n-Bu)}_3(\text{CO})]}{k_{-1}[\text{P(n-Bu)}_3] + k_2[\text{CO}]} \qquad (10)$$

which can be rewritten:

$$\text{rate} = k_f[\text{RuOEP(P(n-Bu)}_3)_2] - k_r[\text{RuOEP(P(n-Bu)}_3)(\text{CO})] \qquad (11)$$

k_f is the overall rate constant for the forward reaction

and k_r is the overall rate constant for the reverse reaction.

This expression can now be integrated[43] to give:

$$(k_f + k_r)t = \ln \frac{A_0 - A_e}{A - A_e} \qquad (12)$$

A_e is the absorbance at the equilibrium position

and A is the absorbance at any time, t.

This then gives the expression:

$$\left(\frac{k_1 k_2 [\text{CO}] + k_{-1}k_{-2}[\text{P(n-Bu)}_3]}{k_{-1}[\text{P(n-Bu)}_3] + k_2[\text{CO}]} \right) t = \ln \frac{A_0 - A_e}{A - A_e} \qquad (13)$$

Plots of $\ln \dfrac{A_0 - A_e}{A - A_e}$ versus time (Figure IV.5) yielded straight lines of

$$\text{slope} = \frac{k_1 k_2 [\text{CO}] + k_{-1}k_{-2}[\text{P(n-Bu)}_3]}{k_{-1}[\text{P(n-Bu)}_3] + k_2[\text{CO}]} = k_{\text{obsd}} \qquad (14)$$

k_{obsd} is the pseudo-first-order rate constant for the reaction.

Table IV.2 gives the kinetic data,
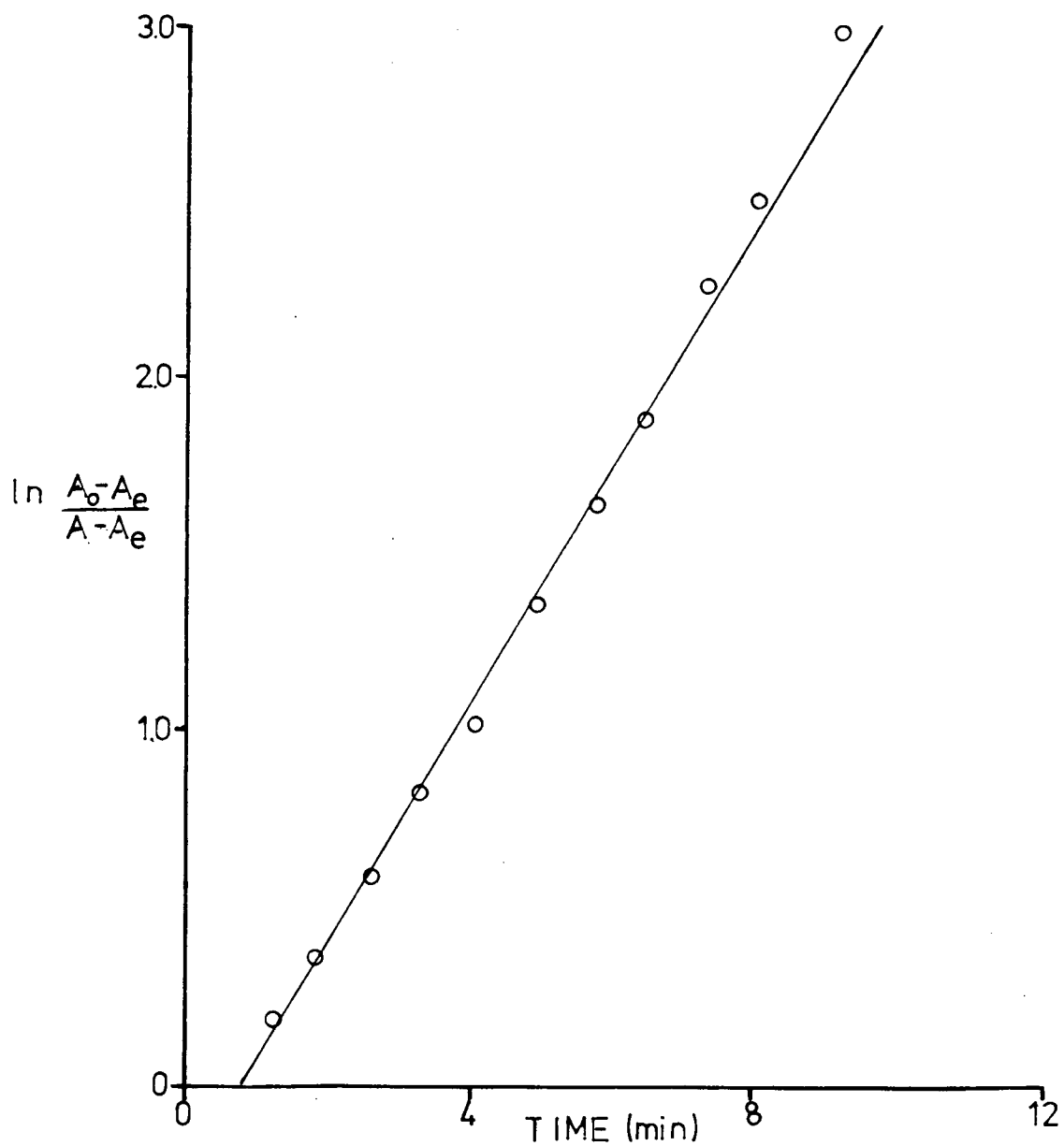
Figure IV.5. First-Order Plot for the Reaction of $RuOEP(P(n-Bu)_3)_2$ with 1 atm CO in toluene containing 7.08×10^{-4} M $P(n-Bu)_3$ at $31^\circ C$.

Table IV.2. <u>Rate of Reaction of RuOEP(P(n-Bu)$_3$)$_2$ with CO in Toluene</u>

   <u>at Various Ligand Concentrations and CO Pressures at 31°C.</u>

CO Pressure[a] (atm)	P(n-Bu)$_3$ (moles/litre)	k_{obsd} x 10^{3b} (sec^{-1})	k_{obsd}(calc)[c] x 10^3 (sec^{-1})
0.971	1.057 x 10^{-3}	6.67	6.08
0.721	1.057 x 10^{-3}	7.77	6.98
0.471	1.057 x 10^{-3}	7.95	7.41
0.221	1.057 x 10^{-3}	11.0	10.45
0.971	7.083 x 10^{-4}	5.67	5.69
0.721	7.083 x 10^{-4}	5.84	5.96
0.471	7.083 x 10^{-4}	6.11	6.59
0.221	7.083 x 10^{-4}	8.75	8.66

a. and b. see Table III.1.
c. see text for explanation, agreement with measured rate
   constants within 10%.

However, due to the complicated nature of the rate law, no simple

graphical method yields the kinetic rate constants. Therefore, alternative

procedures were used.

Since, in the case of RuOEP(P(n-Bu)$_3$)$_2$ and 1 or ½ atmosphere of CO

in toluene with no added phosphine, the reaction went to completion, with

the same measured k_{obsd}, this means that k_1 is rate determining (see

Chap 3). This is thus a direct measure of k_1 (k_1 = 2.11 x 10^{-3} sec^{-1}).

Once such a reaction had been carried to completion, a large excess of

phosphine was added, under the CO atmosphere, and the reaction was pushed

back completely to the left, reforming RuOEP(P(n-Bu)$_3$)$_2$(Table IV.3).

Under these conditions (k_1 being negligible), the rate of the reaction is

$$\text{rate} = \frac{k_{-1}k_{-2}[P(n\text{-}Bu)_3][RuOEP(P(n\text{-}Bu)_3)(CO)]}{k_2[CO] + k_{-1}[P(n\text{-}Bu)_3]} \tag{15}$$

which can be rearranged to give:

$$k_{obsd}^{-1} = k_{-2}^{-1} + k_2[CO]/k_{-1}k_{-2}[P(n-Bu)_3] \tag{16}$$

Therefore, a plot of k_{obsd}^{-1} vs $[CO]/[P(n-Bu)_3]$ should give a straight line of slope $k_2/k_{-1}k_{-2}$ and an intercept of k_{-2}^{-1} (Figure IV.6 and Table IV.4).

Table IV.3. Rate of Reaction of RuOEP(P(n-Bu)$_3$)(CO) With P(n-Bu)$_3$ in Toluene at 31°C.

CO Pressure[a] (atm)	P(n-Bu)$_3$ x 10^2 (moles/litre)	k_{obsd} x 10^{2}[b] (sec^{-1})
0.971	5.02	1.79
0.971	5.73	1.92
0.971	7.15	2.21
0.971	8.57	2.47

a. and b. see Table III.1.

Table IV.4. Kinetic Data For the Reaction of RuOEP(P(n-Bu)$_3$)(CO) and P(n-Bu)$_3$ in Toluene at 31°C.

k_{-1}/k_2[a]	k_{-2}[b] (sec^{-1})
0.061	5.35 x 10^{-2}

a. estimated error ± 10%. b. estimated error ± 25%.

Taking the rate constants listed in Table IV.4 and substituting them back into the expression for k_{obsd} (14) for the overall reaction, rates can be calculated for the conditions listed in Table IV.2 (see table).
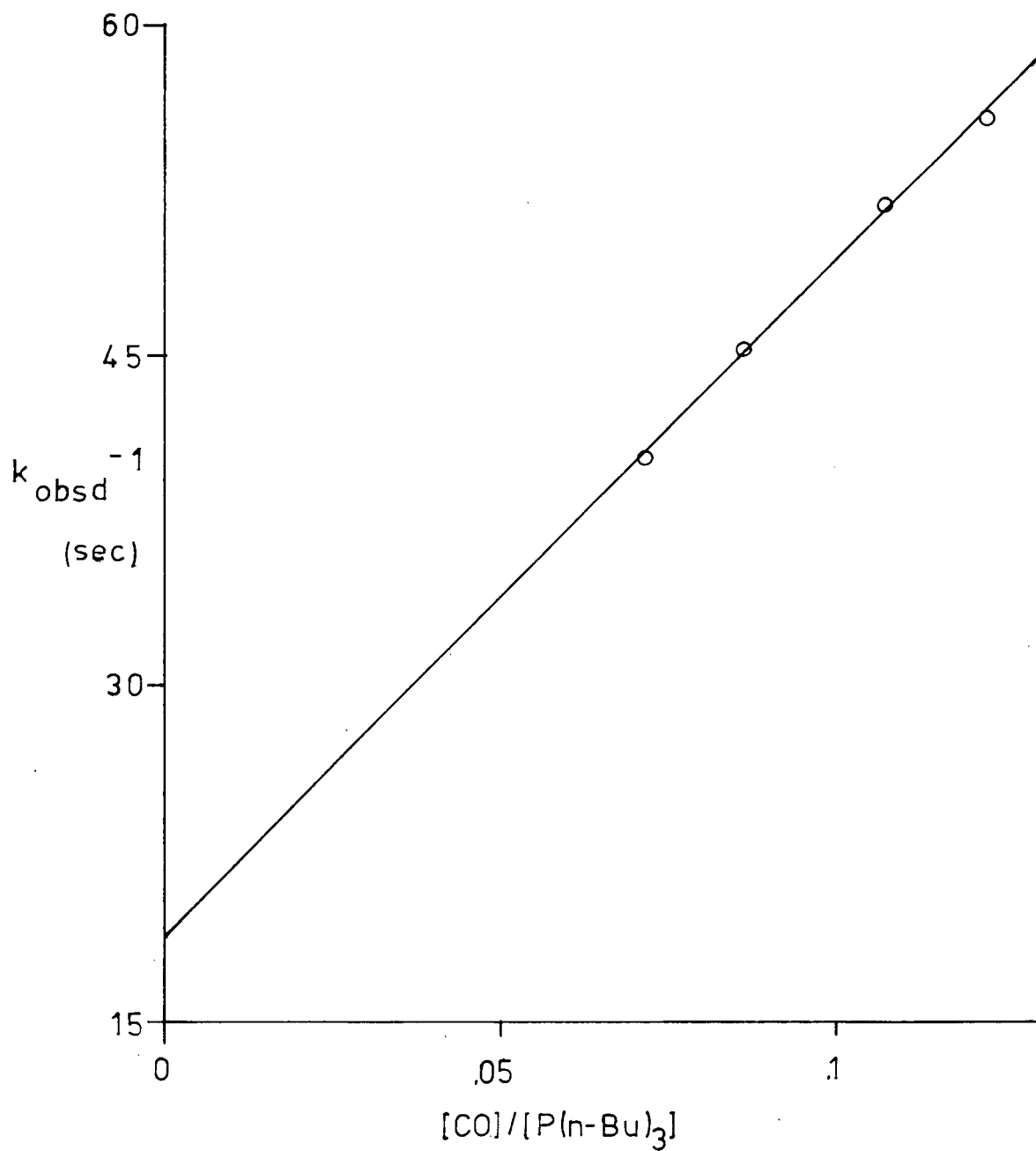
Figure IV.6. Plot of k_{obsd}^{-1} vs $[CO]/[P(n-Bu)_3]$ for the Reaction of RuOEP(P(n-Bu)(CO) with $P(n-Bu)_3$ in Toluene at $31^{\circ}C$.

The complete set of kinetic parameters is listed in Table IV.5. K was calculated by $K = k_1 k_2 / k_{-1} k_{-2}$ and is within 15% of the directly measured K at 31°C.

Table IV.5. Kinetic Data for the Reaction of $RuOEP(P(n-Bu)_3)_2$ and CO at 31°C in Toluene.

k_1 (sec^{-1})	k_{-1}/k_2	k_{-2} (sec^{-1})	K
2.11×10^{-3}	0.061	5.35×10^{-2}	0.647

IV.3 Discussion

From the data, Table IV.5, the six-coordinate bis(phosphine) complex loses a phosphine ligand 25 times slower than the mixed ligand species gives up a CO molecule, very different from the previous bis(acetonitrile) system (see Chap 3). The k_{-1}/k_2 value shows that the five-coordinate intermediate prefers to bind CO over $P(n-Bu)_3$ by a factor of 16, however, the Ru-CO and Ru-$P(n-Bu)_3$ bond strengths are similar (ΔH value).

These data can also be compared to the data of Table III.3. the oxygenation of $RuOEP(pyrrole)_2$ in pyrrole. The k_1 and k_{-1}/k_2 values are quite similar but the k_{-2} value is very different. The off-rate for CO seems to be 1000 times that for oxygen, again quite different to the bis(acetonitrile) system, showing that the phosphine has marked effects on the solution chemistry of the systems.

The data of Table IV.5 can also be compared to those of Table III.2. Though the k_1 and k_{-1}/k_2 values, here too, are very similar, k_{-2} is

very different, resulting in a rather dramatic variation in the value of K. The two k_{-1}/k_2 values differ by a factor of only three which implies that the structure of the five-coordinate $RuOEP(P(n-Bu)_3)$ and $RuOEP(CH_3CN)$ are quite similar(see Chap 3). Further work on the $RuOEPL_2$ systems and other $Ru(porphyrin)L_2$ systems is necessary to get a clearer picture of the nature of the five-coordinate species. At this time, work[44] has started on the study of $RuTPP(CH_3CN)_2$, $RuTPP(phosphine)_2$ and other $RuOEP(phosphine)_2$ systems.

The two k_{-2} values in the systems studied here vary by $\sim10^6$, a very dramatic difference. The phosphine trans to the CO molecule seems to labilize the CO molecule much more readily than an acetonitrile molecule can. Since CH_3CN is not such a good π-acid as $P(n-Bu)_3$[45], the CO is likely to accept more of the π-electron density from the metal centre in the acetonitrile system, therefore strengthening the M-CO bond (solution infrared spectrum taken in hexane, $\sim10^{-3}$ M, $\nu_{CO} = 1935$ cm^{-1}). In the case of the $P(n-Bu)_3$ system, there will be competition for the π-electron density between the $P(n-Bu)_3$ and CO and thus the M-CO bond is not as strong as in the previous case (solution infrared spectrum taken in hexane, $\sim10^{-3}$ M, $\nu_{CO} = 1975$ cm^{-1}) and the CO is now much more easily lost. Such a correlation between CO lability and ν_{CO} seems reasonable for two such closely related systems, but it does not hold more generally[30].

Due to the ease that the RuOEP(phosphine)(CO) system was found to lose a CO molecule, work[46] has been initiated in the area of catalysis in which this system and $RuTPP(phosphine)_2$ species are used to catalytically decarbonylate aldehydes. The main thrust of the work, so far, has been in the use of $RuTPP(P(Ph)_3)_2$ in acetonitrile. A CO atmosphere seems to be

necessary to initiate the decarbonylation reaction. Phenylacetaldehyde has been decarbonylated with turnover numbers of 10^3/hour at 20^oC. However, the actual mechanism of the reaction is far from completely understood.

These ruthenium(porphyrin)(phosphine) systems seem to be quite successful in this area due to the lability of the Ru-CO bond, that results from the presence of the phosphine ligand in the trans axial position. Much more interesting chemistry will probably develop out of these systems in the fields of catalysis and bioinorganic chemistry.

CHAPTER 5

THE REACTIONS OF RuOEP(CH_3CN)_2 WITH OTHER GASES IN TOLUENE

AND WITH CO IN OTHER SOLVENTS

V.1   The Reaction of RuOEP(CH_3CN)_2 With N_2 and With C_2H_4 in Toluene

Since the reaction of $RuOEP(CH_3CN)_2$ in toluene with CO had been

studied, reactions with other gaseous ligands were of interest. Hopf

and Whitten[47] had 'activated' a ruthenium(II) mesoporphyrin IX system by

using surfactant complexes in monolayer assemblies; the system reacted with

CO, O_2 and N_2. Although O_2 was known to oxidize the $RuOEP(CH_3CN)_2$ system

in toluene, it seemed worthwhile investigating its reactivity towards

C_2H_4, isoelectronic with O_2. Its reactivity toward N_2 was also tested.

V.1.1   The Reaction of RuOEP(CH_3CN)_2 and N_2

Toluene solutions of 10^{-5} M $RuOEP(CH_3CN)_2$ with 1.9×10^{-2} M CH_3CN

added were reacted with one atmosphere of N_2 at 30°C; Figure V.1 shows a

'successful' run (see below). The initial spectrum was that of $RuOEP(CH_3CN)_2$

with extinction coefficients stated in Chapter 3. As N_2 reacted, the visible

bands broadened, the final spectrum having a shoulder at 555 nm ($\varepsilon = 1.0$

$\times 10^4$ M^{-1} cm^{-1}) and the main band centred around 525 nm ($\varepsilon = 1.3 \times 10^4$

M^{-1} cm^{-1}). In the Soret region, the band blue shifted to 398 nm ($\varepsilon = 1.67$

$\times 10^5$ M^{-1} cm^{-1}) with small shoulders appearing at 388 nm($\varepsilon = 6.67 \times 10^4$

M^{-1} cm^{-1}) and 378 nm ($\varepsilon = 5.87 \times 10^4$ M^{-1} cm^{-1}).
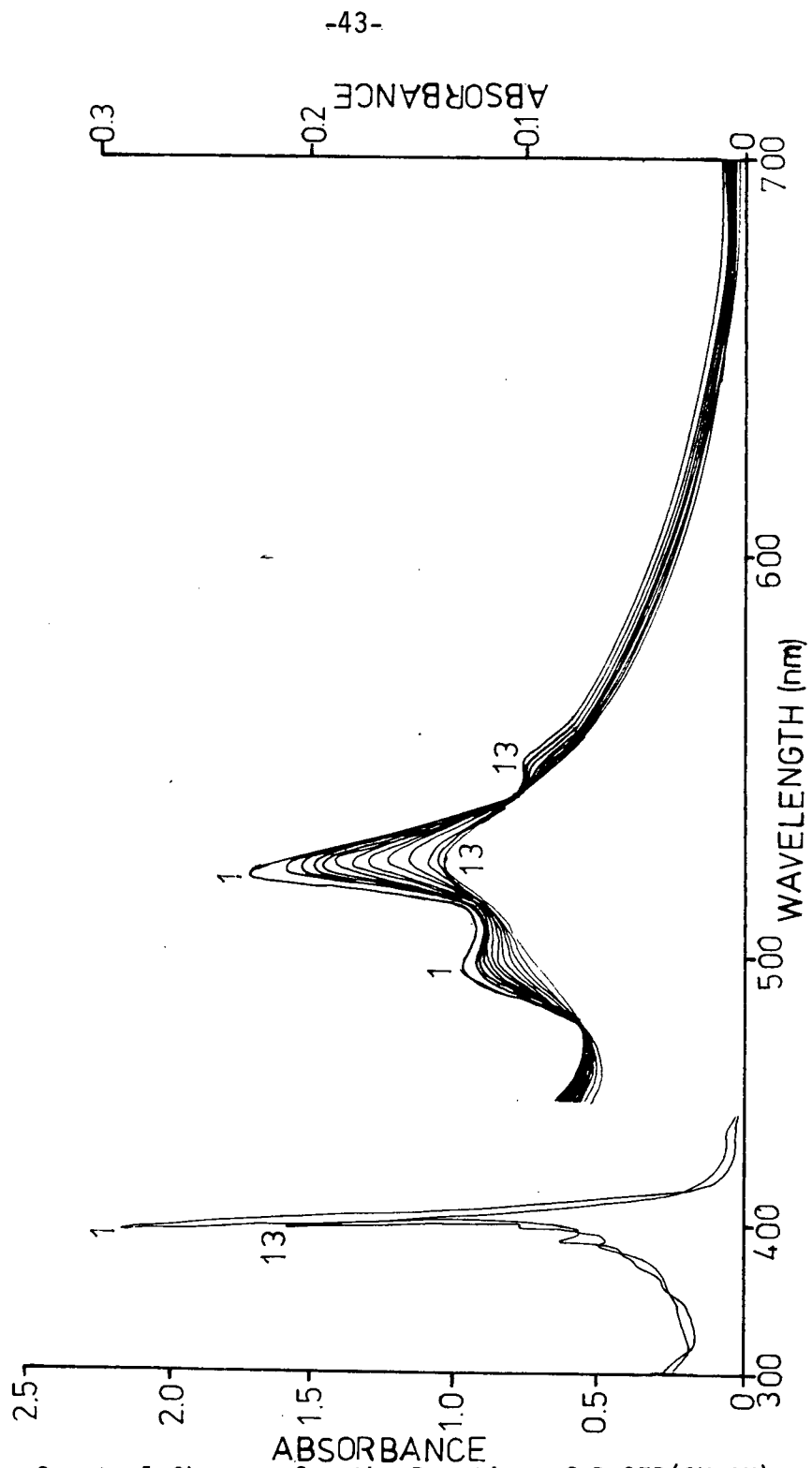
Figure V.1. Spectral Changes for the Reaction of RuOEP(CH$_3$CN)$_2$ with

1 atm N$_2$ in Toluene Containing 1.9 x 10^{-2} M CH$_3$CN at 30°C.

When one atmosphere of N_2 was used in the reaction, the original bands of $RuOEP(CH_3CN)_2$ in the Soret region completely disappeared, suggesting that the reaction had gone to completion. When ½ an atmosphere of N_2 was used, bands from the bis(acetonitrile) species could still be seen. Therefore, an equilibrium process seems to be occurring, presumably:

$$RuOEP(CH_3CN)_2 + N_2 \overset{K}{\rightleftharpoons} RuOEP(CH_3CN)(N_2) + CH_3CN \qquad (17)$$
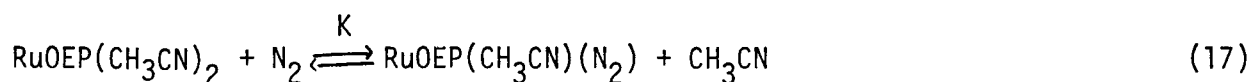
The forward reaction could be partially reversed by freeze-thaw-degassing the solution to remove the N_2.

However, the system proved difficult to study in terms of reproducibility. Many times, while scanning the spectrum during a run, isosbestic points were lost. The collapse of the visible bands was very similar to the reaction of $RuOEP(CH_3CN)_2$ and O_2, in which the product is some oxidized species (see Chap 3). Other times, the reaction would apparently either stop partway through a run or in some cases, never begin at all. Eventually the solution product, thought to be $RuOEP(CH_3CN)(N_2)$ was found to be very light-sensitive and if one wavelength is scanned for too long, some of the N_2 will photolyze off the complex to regenerate the $RuOEP(CH_3CN)_2$ species.

Of the reactions with good isosbestic points, inconsistent kinetic data were obtained. For example, though good first-order plots were obtained (Figure V.2) for the reaction of $RuOEP(CH_3CN)_2$ with one atmosphere of N_2 at $30^{\circ}C$ (from data obtained by monitoring the decrease in intensity of the 525 nm band) pseudo-first-order rate constants from 5.70×10^{-4} sec^{-1} to 2.14×10^{-4} sec^{-1} were obtained.

Therefore, the study of this particular system was abandoned.
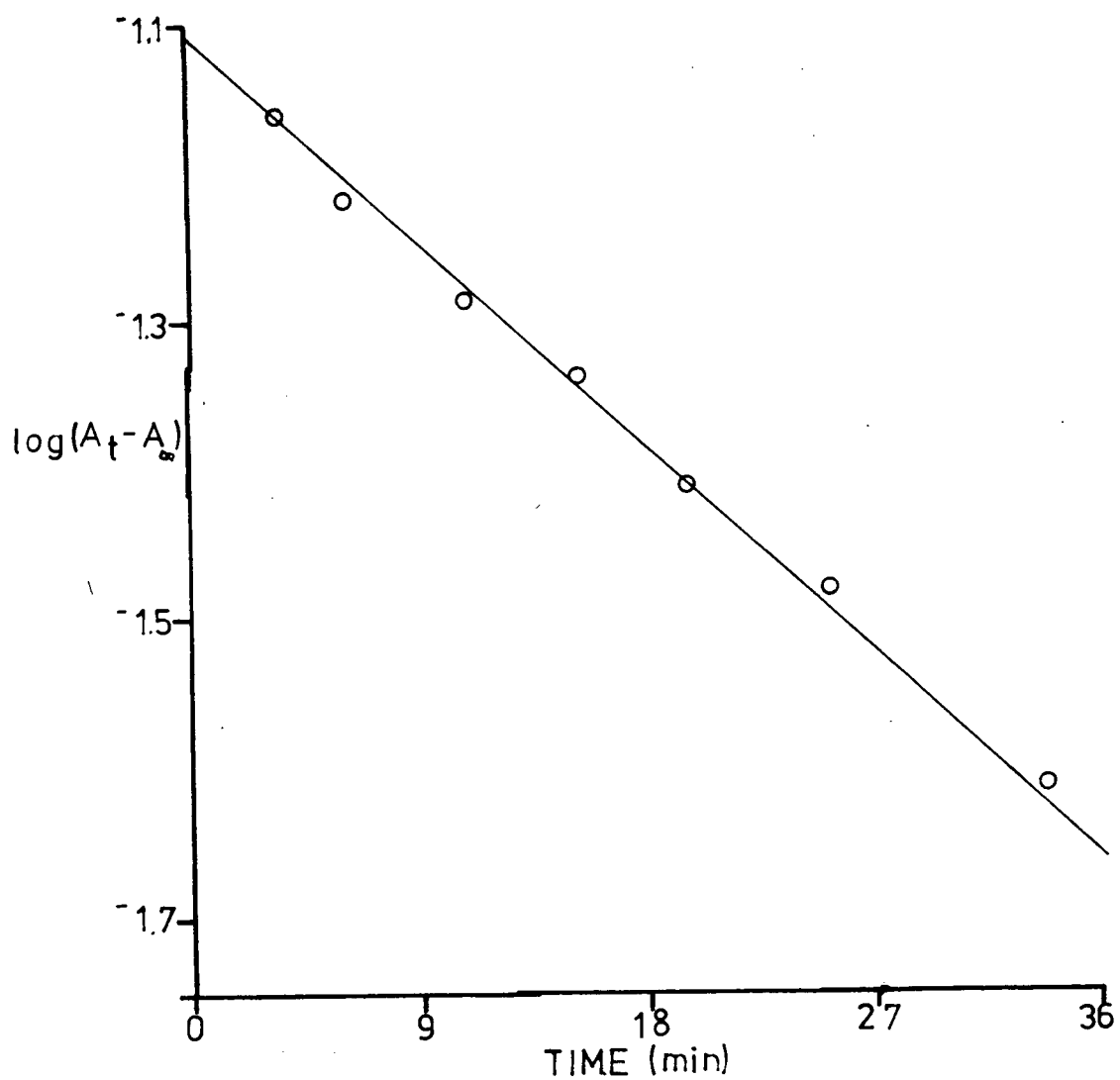
Figure V.2. First-Order Plot for the Reaction of RuOEP(CH$_3$CN)$_2$ with

1 atm N$_2$ in Toluene Containing 1.9 x 10^{-2} M CH$_3$CN at 30°C.

The light sensitivity coupled with possible trace oxygen impurities rendered the system impractical to study from a kinetic viewpoint.

Closely related work[39] has been done in this laboratory in another solvent, tetrahydrofuran (THF), in which N_2 also seems to bind to a ruthenium porphyrin complex. By photolyzing $RuOEP(CO)(EtOH)$ in THF, $RuOEP(THF)_2$ is formed in situ. The THF was evaporated off by bubbling N_2 through the solution and a red solid was isolated which is believed to be the N_2 adduct, $RuOEP(THF)(N_2)$. The solid had a $\nu_{N_2} = 2110$ cm^{-1}, which can be compared to a $\nu_{N_2} = 2088$ cm^{-1} for the complex trans-$[Ru(NH_3)_4(H_2O)(N_2)]^{2+}$ [48]. However, no kinetic studies have been carried out on this system.

V.1.2 The Reaction of $RuOEP(CH_3CN)_2$ With C_2H_4

Toluene solutions of 10^{-5} M $RuOEP(CH_3CN)_2$ with 1.9×10^{-2} M CH_3CN added were reacted with 3/4 atmosphere of C_2H_4 at 30°C(Figure V.3). Again, from examining the bands in the Soret region, the reaction appears to have gone to completion. The spectrum of the final product is very similar to that of the proposed $RuOEP(CH_3CN)(N_2)$ species, showing a broad band in the visible region. The final spectrum has a shoulder at 548 nm ($\varepsilon = 9.24 \times 10^3$ M^{-1} cm^{-1}), a broad band centred around 525 nm ($\varepsilon = 1.18 \times 10^4$ M^{-1} cm^{-1}) and in the Soret region, a main band at 398 nm ($\varepsilon = 2.04 \times 10^5$ M^{-1} cm^{-1}) with shoulders at 388 nm ($\varepsilon = 9.37 \times 10^4$ M^{-1} cm^{-1}) and at 378 nm ($\varepsilon = 6.77 \times 10^4$ M^{-1} cm^{-1}). Some reversal of the reaction could be seen by degassing the solvent.

As with the case of binding N_2, the kinetic runs were very inconsistent. Often the spectral curves would lose their isosbestic points partway through the reaction, and sometimes the reaction would
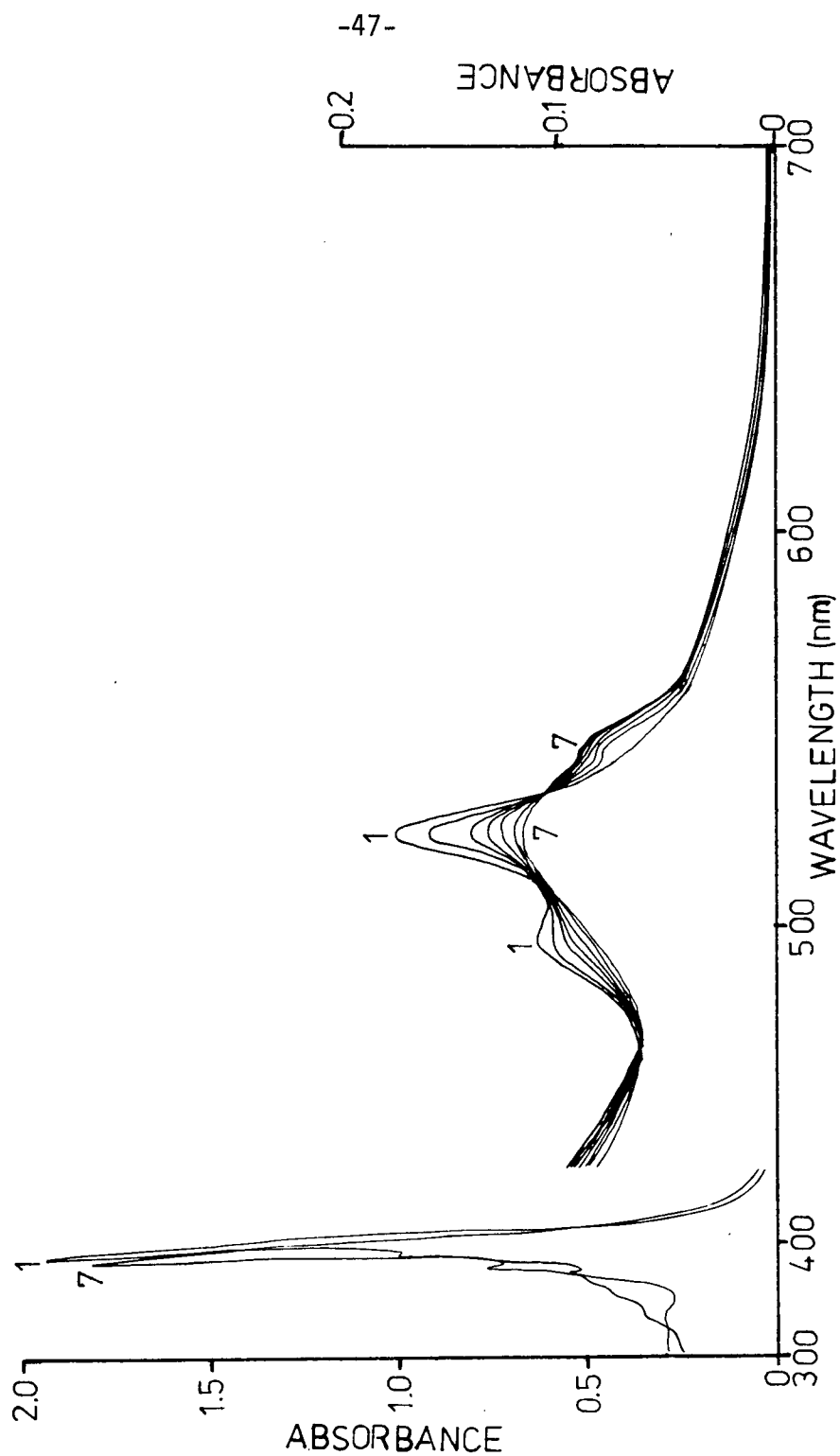
Figure V.3. Spectral Changes for the Reaction of $RuOEP(CH_3CN)_2$ with 3/4 atm of C_2H_4 in Toluene Containing 1.9×10^{-2} M CH_3CN at $30^{\circ}C$.

never start at all.

When the initial amount of added CH_3CN was doubled to 0.038 M and spectral changes were observed, the extent of C_2H_4 binding seemed to be very small, consistent with some sort of equilibrium such as:

$$RuOEP(CH_3CN)_2 + C_2H_4 \xoverset{K}{\rightleftharpoons} RuOEP(CH_3CN)(C_2H_4) + CH_3CN \qquad (18)$$
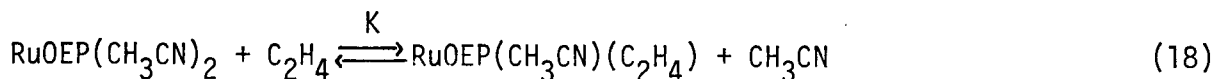
This reaction, as in the N_2 reaction, seemed to be extremely photo- and oxygen-sensitive, the C_2H_4 not being bound very tightly. The use of tetracyanoethylene, TCNE, was considered because activated olefins should coordinate more strongly and stabilize any Ru-olefin complex. However, TCNE in toluene produced intense colours due to the formation of a charge-transfer complex[49]; the intense colour covers the absorption bands of the porphyrin complex in the visible region.

Reversible binding of C_2H_4 to $RuOEP(THF)_2$ in THF at 20°C has also been demonstrated by spectroscopy by another worker in this laboratory[39].

The exact nature of the ethylene complex is of particular interest. The species presumably contains a π-bonded olefinic moiety but it is not known whether one or both CH_3CN ligands come off when the C_2H_4 is bound:

i.e.

        3   4
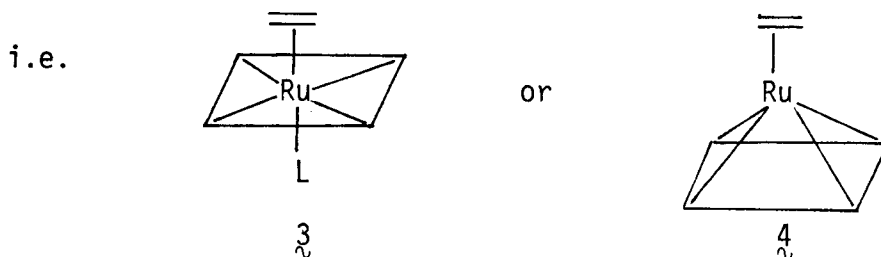
Figure V.4 Possible structures for ethylene complex.

Complex 3 is considered as formally seven-coordinate. A Mn(II) porphyrin system that binds O_2 (and TCNE) does lose an axial ligand in forming

complexes of type $\underset{\sim}{4}$[13b].

Information on the ruthenium system could relate back to the ruthenium complexes that bind oxygen. There is no report of any metal centre that binds both dioxygen as an end-on superoxide and also π-bonded ethylene. Ethylene complexes are usually formed with systems that give peroxides[4,50] (eg. Rh^I, Ir^I, Pt^0). The evidence suggests then that perhaps instead of binding dioxygen as a bent superoxide ($Ru^{III}-O_2^-$), the O_2 is bound as a side-on peroxide ($Ru^{IV}-O_2^{-2}$) with the ruthenium being formally in the +4 oxidation state. One isolated Ru(IV) complex, $H_4Ru(P(Ph)_3)_3$, has been found[51] to be seven-coordinate.

Unfortunately, an oxygenated ruthenium porphyrin complex has not been isolated yet and due to the noted inconsistencies, no further work was done on the ethylene binding by $RuOEP(CH_3CN)_2$ in toluene.

V.2 The Reaction of $RuOEP(CH_3CN)_2$ With CO in Other Solvents

Since the reaction of $RuOEP(CH_3CN)_2$ and CO in toluene had gone so cleanly, the same reaction in other solvents was also tried, particularly since the reversible O_2-binding had been demonstrated[31] in the aprotic, polar solvents DMA, DMF and pyrrole. On dissolving the $RuOEP(CH_3CN)_2$ complex in the coordinating solvents used, (DMF, DMA, THF, py and pyrrole), both CH_3CN ligands were believed to be displaced by the solvent ligands (see below). The bis species could certainly be formed in situ by photolyzing the RuOEP(CO)(EtOH) adduct in the appropriate solvent (see Experimental), but then there was always the possibility of some dissolved CO remaining in the solvent, and this could possibly have interfered with the CO reaction being studied. The only useful isolated solid was $RuOEP(CH_3CN)_2$, and since acetonitrile ligands are fairly labile (as

judged by the reaction with CO in toluene-Chap. III), the solvent ligands, at sufficiently high concentrations, should easily displace the acetonitrile, whose concentration would be low (twice that of the Ru-porphyrin) and not interfere with the CO reaction to be studied.

V.2.1 The Reaction of RuOEP(CH₃CN)₂ With CO in Pyridine (py).

The $RuOEP(CH_3CN)_2$ complex in neat pyridine gives the bis(pyridine) species, but the system is completly unreactive towards CO, which is quite consistent with a dissociative mechanism involving initial loss of a pyridine ligand.

Dissolution of $RuOEP(CH_3CN)_2$ in toluene containing 0.15 M pyridine, again, gave a spectrum similar to that reported[52] for solid $RuOEP(py)_2$ in benzene. Visible bands appear at 521 nm ($\varepsilon = 3.80 \times 10^4$ M^{-1} cm^{-1}), 495 nm ($\varepsilon = 1.48 \times 10^4$ M^{-1} cm^{-1}), 450 nm ($\varepsilon = 1.58 \times 10^4$ M^{-1} cm^{-1}) and a Soret band at 395 nm ($\varepsilon = 1.02 \times 10^5$ M^{-1} cm^{-1}). However, under these conditions, based on the known spectrum of $RuOEP(CO)(py)$[52] (solid prepared by a method similar to that of RuOEP(CO)(EtOH)-see Experimental), the reaction of the $RuOEP(py)_2$ with one atmosphere of CO at 25°C was only ∿15% complete after 3 days (Figure V.5). This would give K for the reaction (19) at 25°C as ∿25, some 50 times greater than for the analogous $RuOEP(P(n-Bu)_3)_2$ system; this could reflect the stronger Ru-CO bond of the pyridine system due to the weaker π-acceptor[45] properties of the trans pyridine compared to the phosphine.

$$RuOEP(py)_2 + CO \overset{K}{\rightleftharpoons} RuOEP(CO)(py) + py \qquad (19)$$
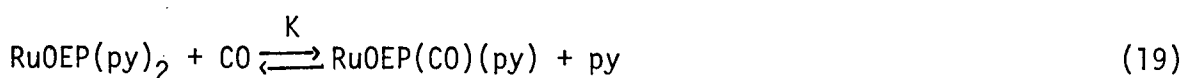
Surprisingly, toluene solutions of the bis(acetonitrile) complex containing 0.015 M pyridine did not completely form the bis(pyridine)

Figure V.5. Spectral Changes for the Reaction of $RuOEP(CH_3CN)_2$ with 1 atm CO in Toluene Containing 0.15 M pyridine at $25^{\circ}C$.
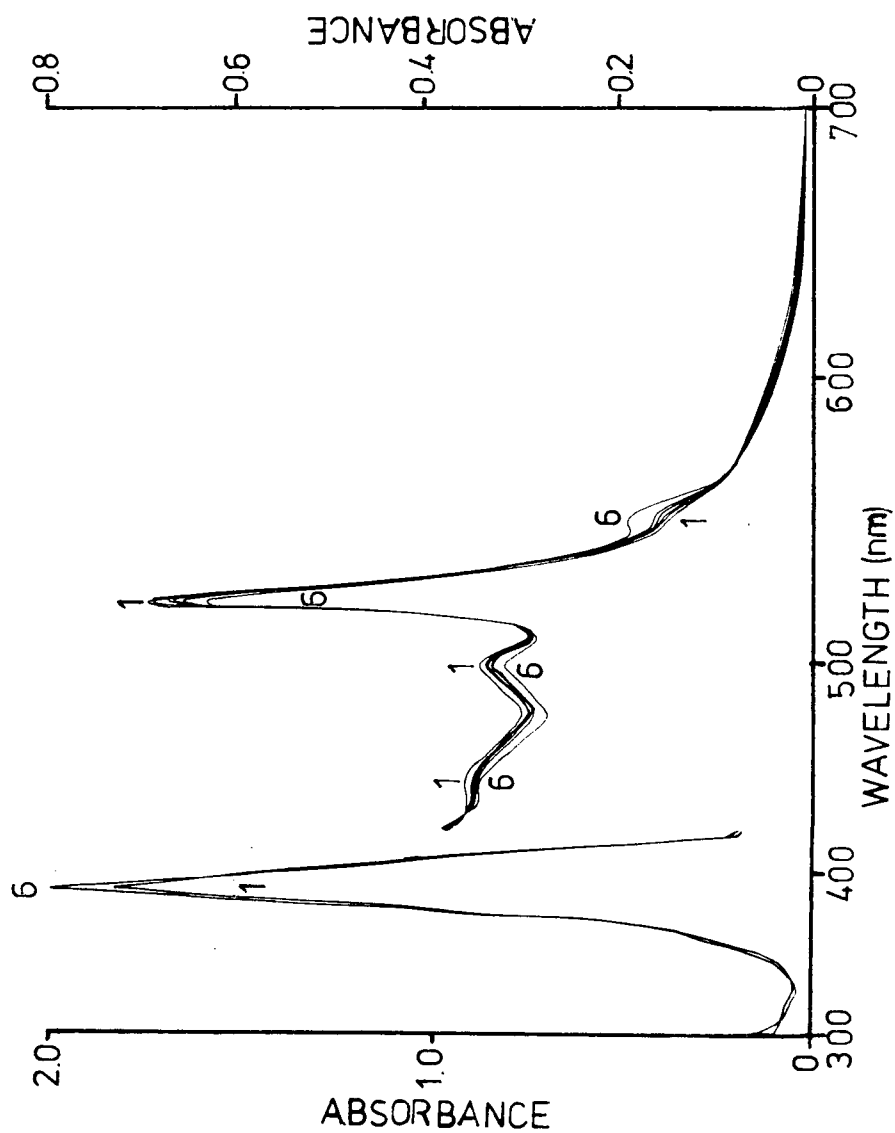
species, which has a characteristic band at 450 nm. Presumably, the mixed ligand species RuOEP(CH$_3$CN)(py) must be present. Studies on the pyridine systems were not pursued further partially due to this added complication.

V.2.2 The Reaction of RuOEP(CH$_3$CN)$_2$ With CO in N,N-Dimethylacetamide (DMA), N,N-Dimethylformamide (DMF) and Tetrahydrofuran (THF).

Since the solid RuOEP(DMA)$_2$ has not been isolated, the species was formed in situ by photolyzing a 10^{-5} M solution of the RuOEP(CO)(EtOH) complex in DMA for ∿2 min. Spectral bands were found at 521 nm (ε =3.52 x 10^4 M^{-1} cm^{-1}), 498 nm (ε = 1.15 x 10^4 M^{-1} cm^{-1}) and 395 nm (ε = 1.68 x 10^5 M^{-1} cm^{-1}). The RuOEP(CO)(DMA) species, which is considered to be formed when RuOEP(CO)(EtOH) is dissolved in DMA, has bands at 548 nm (ε = 2.90 x 10^4 M^{-1} cm^{-1}), 517 nm (ε = 1.49 x 10^4 M^{-1} cm^{-1}), 394 nm (ε = 2.16 x 10^5 M^{-1} cm^{-1})and a shoulder at 373 nm (ε = 3.85 x 10^4 M^{-1} cm^{-1}) (Figure V.6).

Of interest, when the solid RuOEP(CH$_3$CN)$_2$ is dissolved in DMA, a spectrum (trace #1 on Figure V.7) different to that of RuOEP(DMA)$_2$ is observed. The visible bands of this species 'X' are much broader and the band at 521 nm is only 1.4 times more intense than the 498 nm band; the ratio of these band intensities in the bis(DMA) species is about 3. The spectrum resembles the type of spectrum normally attributed to a five-coordinate species (Chapter 3). If this solution is photolyzed for ∿2 min, the bis(DMA) species can be generated but this gradually collapses back to the species 'X' spectrum. The acetonitrile must be playing a role, and, as in the pyridine system, a mixed species, in this case, RuOEP(CH$_3$CN)(DMA), is strongly indicated. The possibility of

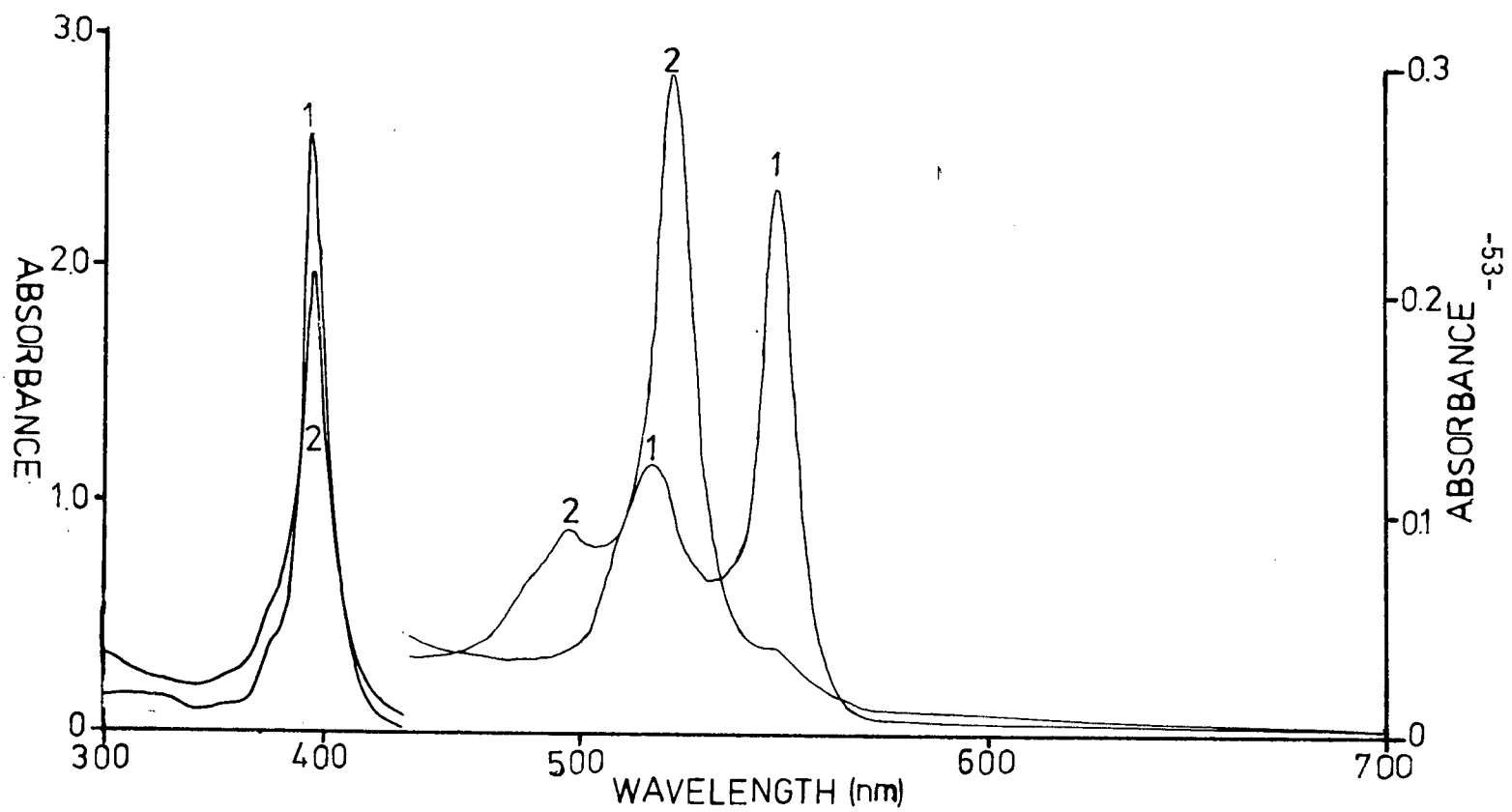Figure V.6. Spectral Changes for the Photolysis of RuOEP(CO)(DMA) forming RuOEP(DMA)₂ in DMA.
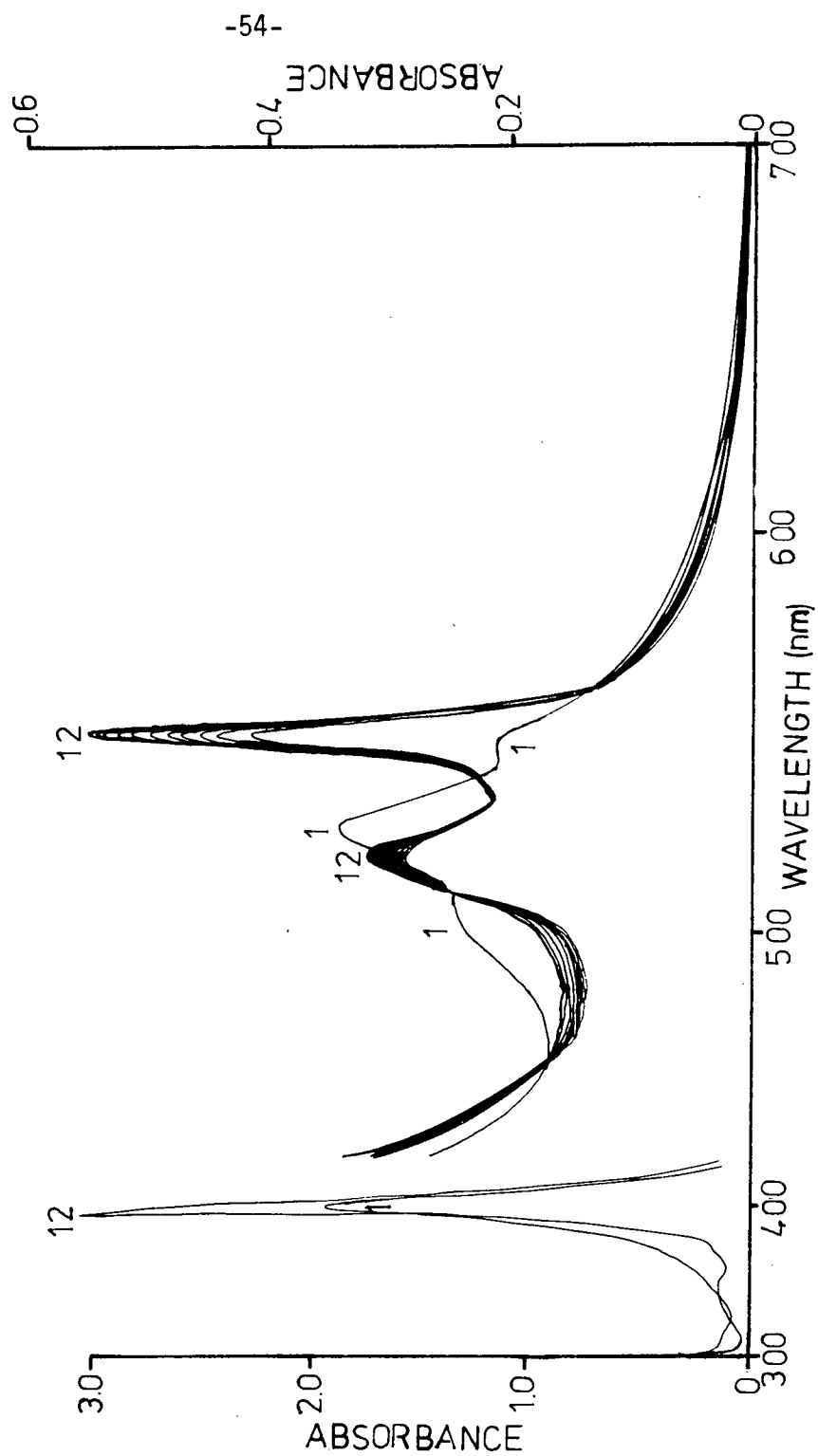
Figure V.7. Spectral Changes for the Reaction of Species 'X' with 1 atm CO in DMA at 29°C.

π-bonded acetonitrile cannot be completely ruled out[53].

When one atmosphere of CO is added to the RuOEP(DMA)$_2$ species, formed in situ, there is an immediate spectral change to one that is identical to that of the RuOEP(CO)(DMA) species which is stable as such. When species 'X' is reacted with one atmosphere of CO, there is again an 'instantaneous' spectral change, but this is followed by a series of slower spectral changes that also yield isosbestic points over a period of several hours (Figure V.7), the final spectrum resembling that of RuOEP(CO)(DMA). A plot of log(A_t-A_∞) versus time, for the slower changes, based on the increase in intensity of the 548 nm band, gives a straight line (Figure V.8) of slope = 1.09 x 10^{-4} sec^{-1} at 29°C. When RuOEP(CH$_3$CN)$_2$ was dissolved in toluene containing 0.21 M DMA, the same initial broad spectrum of species 'X' was achieved and when one atmosphere of CO was added to the solution, the same sort of spectral changes, as those illustrated in Figure V.7, occurred. A first-order plot also gave a straight line of slope = 1.03 x 10^{-4} sec^{-1}, which suggests that the measurable, slower part of the reaction is independent of the amount of DMA present. Further, when species 'X' in neat DMA was reacted with 3/4 atmosphere of CO, the rate decreased to 7.43 x 10^{-5} sec^{-1}, indicating a first-order dependence on CO.

As to what is actually occurring in solution is still unknown. There is a very fast reaction, followed by a much slower reaction. The data suggest that first one species is formed rapidly in solution and this slowly rearranges or reacts further with the CO, both reactant and product species having visible and Soret bands in the same positions.

The second, slower step could be the formation of a bis(carbonyl) species. There has been a report[54] of the formation of the bis(carbonyl)

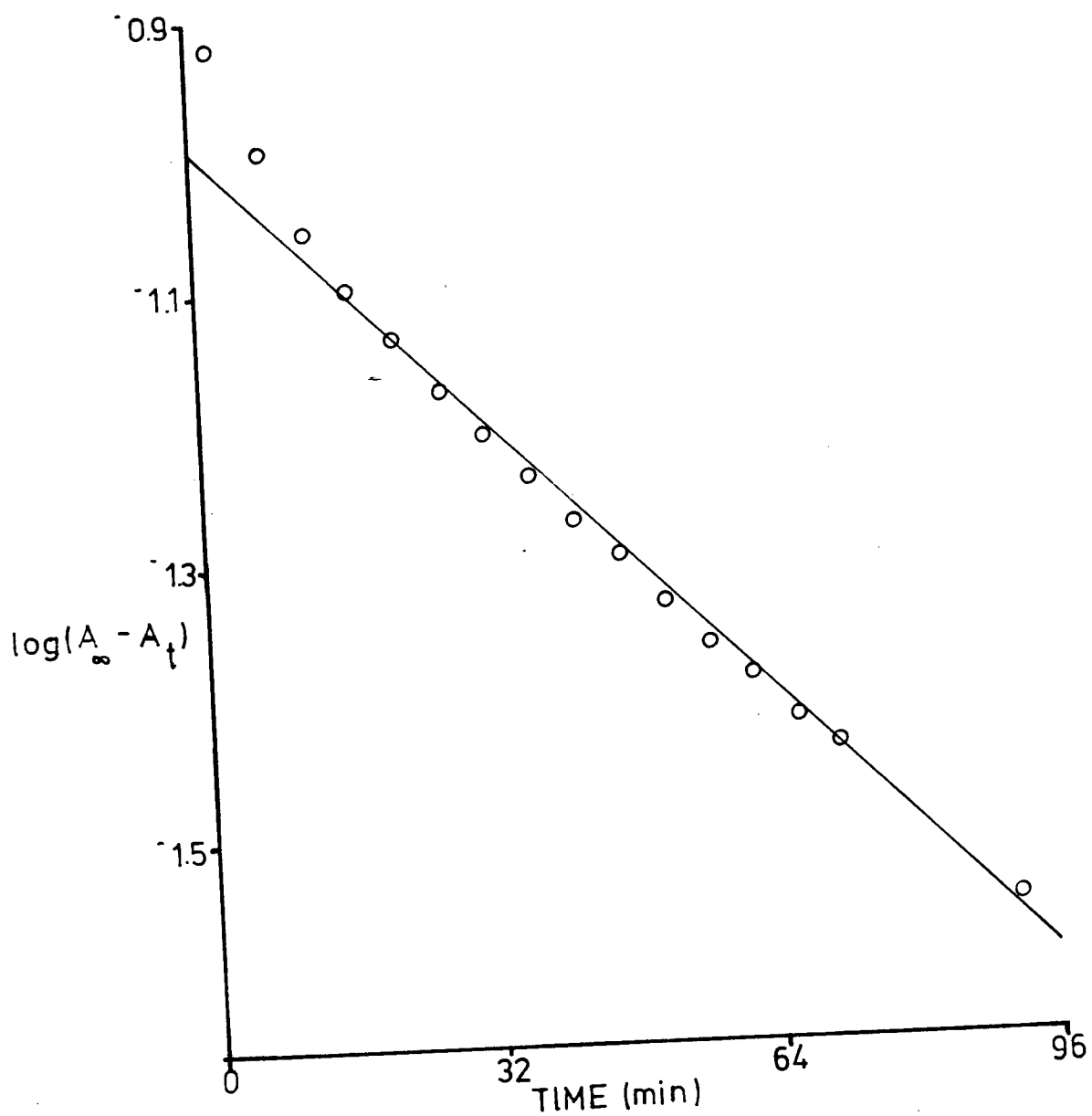Figure V.8. First-Order Plot of the Reaction of Species 'X' with 1 atm CO in DMA at 29°C.

complex of RuOEP in benzene. The complex precipitates out of solution when CO is bubbled through a benzene solution of RuOEP(CO)(EtOH). The trans carbonyls give rise to a ν_{CO} = 1990 cm^{-1}, higher than that of the mono-carbonyl. Attempts made to get a solution infrared spectrum of the product from the slow reaction were unsuccessful, since DMA absorbs very strongly in this region. Work[55] has been done recently within the Bioinorganic Group on the RuOEP(CO)$_2$ complex. A visible spectrum can only be obtained in a non-coordinating solvent, since one CO molecule is rapidly replaced in a coordinating solvent such as DMA, pyridine, etc. The visible spectrum of the bis(carbonyl) species in toluene differs from the monocarbonyl (EtOH adduct) in toluene in that the 548 nm band sharpens and intensifies slightly and the 517 nm band develops hyperfine side bands at 508 nm and 513 nm. At room temperature, toluene solutions of the bis(carbonyl) species are not stable with respect to loss of CO and spectral studies must be carried out at sub-zero temperatures. Considering these facts, a second CO molecule adding on to 'RuOEP(CO)(DMA)' at 29°C in DMA to give RuOEP(CO)$_2$ seems highly unlikely.

If species 'X' or RuOEP(DMA)$_2$ is left in DMA for long periods, the species will abstract CO from the solvent. When RuOEP(DMA)$_2$ is formed in situ and the solution is thoroughly degassed and left under argon, over a period of 24 hours there is a gradual increase in intensity of the band at 548 nm and a large decrease in intensity of the 521 nm and 498 nm bands; the changes appear consistent with formation of RuOEP(CO)(DMA). There have been other reports[56] of ruthenium complexes abstracting CO from DMA.

DMF was also studied as a solvent system. The RuOEP(DMF)$_2$ species formed is situ was found to have bands at 521 nm (ϵ = 5.38 x 10^4 M^{-1} cm^{-1}),

493 nm (ε = 1.97 x 10^4 M^{-1} cm^{-1}) and 391 nm (ε = 2.29 x 10^5 M^{-1} cm^{-1}).
The RuOEP(CO)(DMF) species formed from the carbonyl-ethanol adduct
dissolved in DMF has bands at 548 nm (ε = 3.60 x 10^4 M^{-1} cm^{-1}), 517 nm
(ε = 2.44 x 10^4 M^{-1} cm^{-1}), 394 nm (ε = 2.96 x 10^5 M^{-1} cm^{-1}) and a shoulder
at 374 nm (ε =6.00 x 10^4 M^{-1} cm^{-1}). Again, when RuOEP(CH_3CN)$_2$ is dissolved
in DMF, a species different to RuOEP(DMF)$_2$ is attained and this reacts
with one atmosphere of CO as seen in Figure V.9. The reaction is similar to
that which occurred in DMA. There is rapid initial spectral changes
followed by a slow reaction which takes $\sim$12 hours to go to completion
with a rate constant of 1.9x10^{-5} sec^{-1} at 29°C.

The corresponding study in THF gave very similar findings. The
RuOEP(THF)$_2$ species has bands at 521 nm (ε = 6.84 x 10^4 M^{-1} cm^{-1}), 494 nm
(ε = 2.03 x 10^4 M^{-1} cm^{-1}), 388 nm (ε = 2.55 x 10^5 M^{-1} cm^{-1}) and 296 nm
(ε = 7.87 x 10^4 M^{-1} cm^{-1}). The RuOEP(CO)(THF) species has bands at 549 nm
(ε = 4.10 x 10^4 M^{-1} cm^{-1}), 518 nm (ε = 2.60 x 10^4 M^{-1} cm^{-1}), 396 nm
(ε = 4.98 x 10^5 M^{-1} cm^{-1}) and a broad band at $\sim$320 nm (ε = 3.89 x 10^4
M^{-1} cm^{-1}). When the RuOEP(CH_3CN)$_2$ was dissolved in the THF (the THF had to
be distilled on the vacuum line, directly into the cell, avoiding any
contact with air) a broad spectrum was once again achieved. The addition
of one atmosphere of CO yielded again a two-step reaction (Figure V.10).
The slower reaction was complete in $\sim$30 minutes with a rate constant of
6.45 x 10^{-4} sec^{-1} at 30°C.

When the DMA, DMF and THF systems, the species 'X' present on
dissolution of RuOEP(CH_3CN)$_2$ in any of these solvents could be converted
into the RuOEP(solvent)$_2$ species by less than 2 minutes of photolysis.
Also, the RuOEP(solvent)$_2$ species react very quickly (less than 2 minutes)
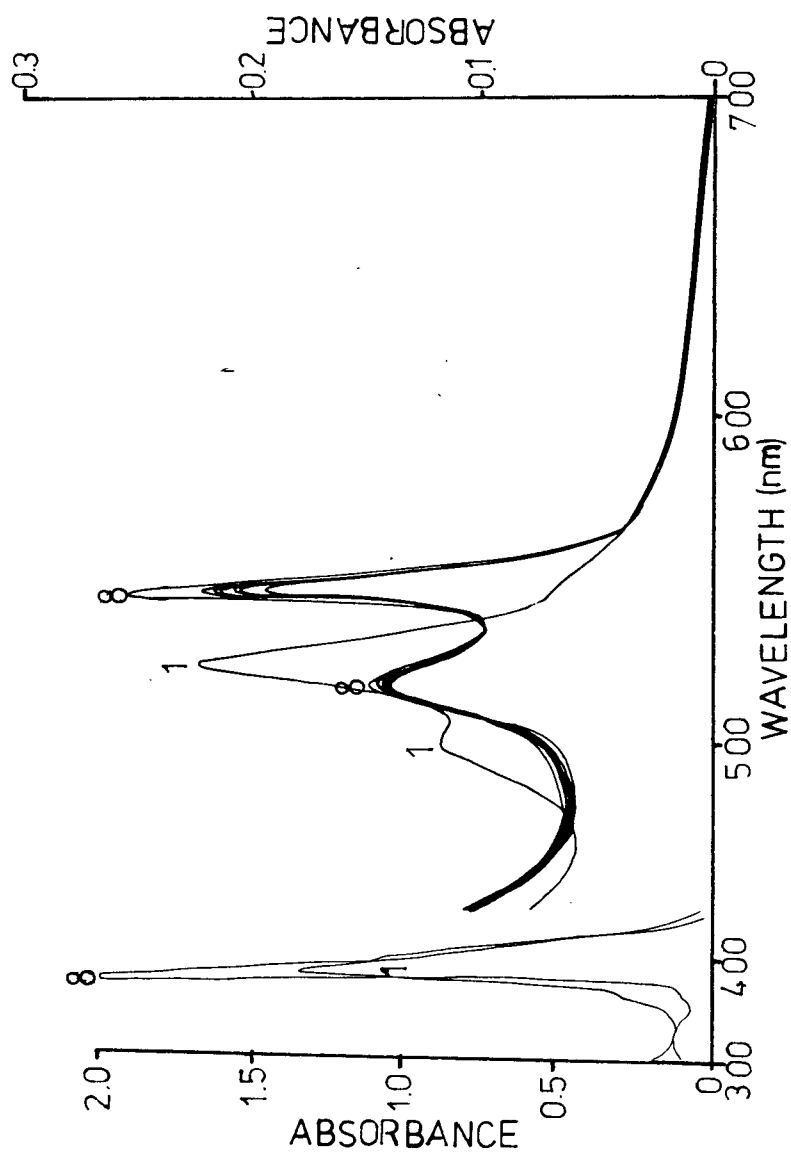
Figure V.9. Spectral Changes for the Reaction of Species 'X' with 1 atm CO in DMF at 29°C.
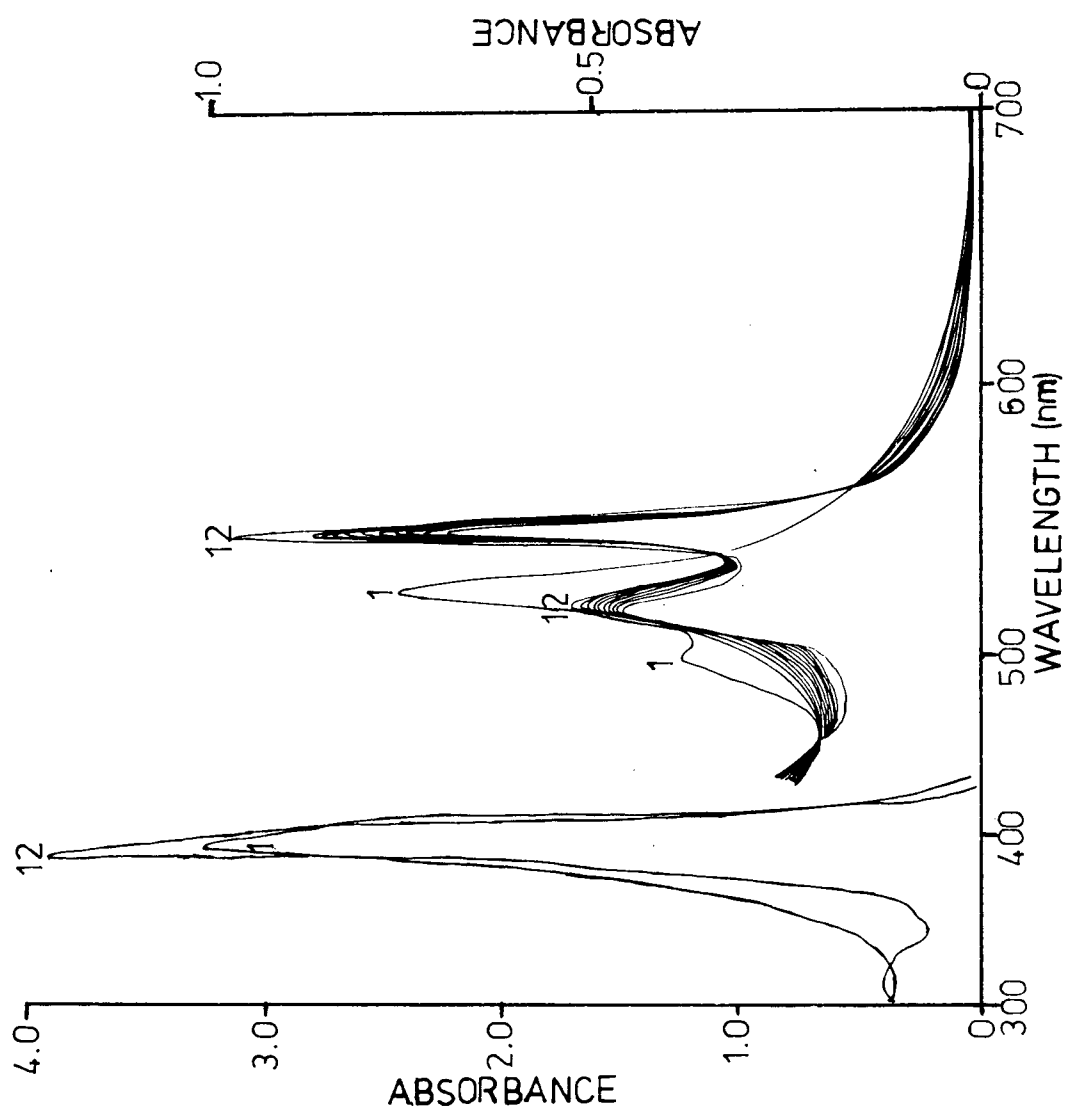
Figure V.10. Spectral Changes for the Reaction of Species 'X' with
1 atm CO in THF at 30°C.

with one atmosphere of CO to give the RuOEP(CO)(solvent) spectrum, while the corresponding species 'X' react quite differently.

One thing these solvents have in common is that they are susceptible to metal-catalyzed decarbonylation[56-58], which may be more than a coincidence. It is unlikely that 'X' is a carbonyl, since the spectra are more typical of RuOEP(L)$_2$ rather than RuOEP(CO)L. Species 'X' is most likely RuOEP(CH$_3$CN)(solvent). As mentioned in Chapter 4, the bis(phosphine) ruthenium porphyrin complexes have been found to catalytically decarbonylate aldehydes, and this was initiated by exposure to CO with subsequent very high turn-over numbers for the catalysis[46]. It is feasible that the initial exposure of RuOEP(CH$_3$CN)(solvent) to CO could give rapid decarbonylation of the solvent to give an amine (at least in the cases of DMA and DMF). The product would likely be, for the DMA system, RuOEP(CO)(N(CH$_3$)$_3$), and the spectrum after the rapid CO reaction is that of a carbonyl. The subsequent slow step could then be replacement of the amine by the solvent ligand. The suggested scheme is outlined below using DMA as the solvent system:

$$\text{RuOEP(CH}_3\text{CN)}_2 + \text{DMA} \rightleftharpoons \text{RuOEP(CH}_3\text{CN)(DMA)} \xrightarrow[\text{fast}]{\text{CO}} \text{RuOEP(CO)(N(CH}_3)_3)$$

$$h\nu \updownarrow \text{slow} \qquad\qquad \downarrow \text{slow}$$

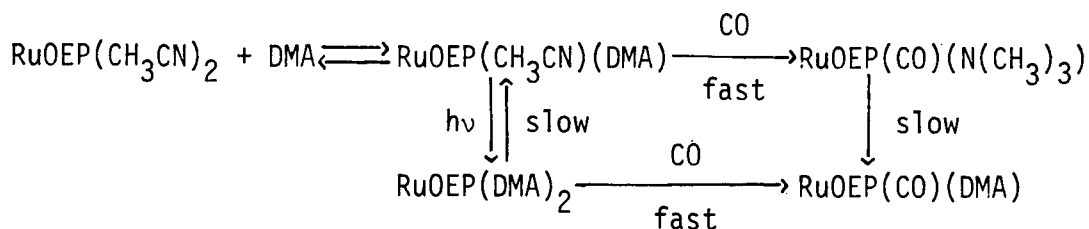$$\text{RuOEP(DMA)}_2 \xrightarrow[\text{fast}]{\text{CO}} \text{RuOEP(CO)(DMA)}$$

Figure V.11. Possible scheme to explain the observed spectral changes of RuOEP(CH$_3$CN)$_2$ with CO in DMA, DMF and THF.

The spectrophotometric data could be consistent with such a scheme. The

minimal kinetic data indicate that the slow step is first-order in CO, and this is difficult to rationalize, however, since the slow spectral changes look very much like the conversion of one monocarbonyl into another. More work needs to be done on these systems before this series of reactions can be fully understood.

V.2.3 The Reaction of $RuOEP(CH_3CN)_2$ With CO in Pyrrole.

Since some of the original reversible oxygenation work[31] was done in pyrrole, this was also tried as a solvent for the reaction with CO. As in the case of the DMA, DMF and THF systems, the species 'Y' obtained when $RuOEP(CH_3CN)_2$ is dissolved in pyrrole is not the $RuOEP(pyrrole)_2$ species. $RuOEP(pyrrole)_2$ has bands at 522 nm($\varepsilon = 3.25 \times 10^4$ M^{-1} cm^{-1}), 495 nm ($\varepsilon = 1.61 \times 10^4$ M^{-1} cm^{-1}) and 395 nm ($\varepsilon = 1.09 \times 10^5$ M^{-1} cm^{-1}). The carbonyl, $RuOEP(CO)(pyrrole)$, has bands at 550 nm ($\varepsilon = 2.05 \times 10^4$ M^{-1} cm^{-1}), 518 nm ($\varepsilon = 1.36 \times 10^4$ M^{-1} cm^{-1}), 397 nm ($\varepsilon = 2.23 \times 10^5$ M^{-1} cm^{-1}), a shoulder at 375 nm ($\varepsilon = 4.01 \times 10^4$ M^{-1} cm^{-1}) and a broad band at ~310 nm ($\varepsilon = 6.76 \times 10^4$ M^{-1} cm^{-1}).

Species 'Y' has a less intense and broader Soret band than the bis(pyrrole) complex and a difference in peak height ratios in the visible region. When one atmosphere of CO was added to species 'Y' there is now no sudden spectral change; gradual changes occur as a function of time and excellent isosbestic points are noted (Figure V.12). The reaction at $30^\circ C$ appears to be ~70% complete in an hour but the solution had to be left overnight to get a final spectrum and when less than one atmosphere is used, the reaction is less complete suggesting a reversible equilibrium. When a first-order plot was done for the reaction with one atmosphere (Figure V.13), though, the log plot starts out in a linear fashion, but
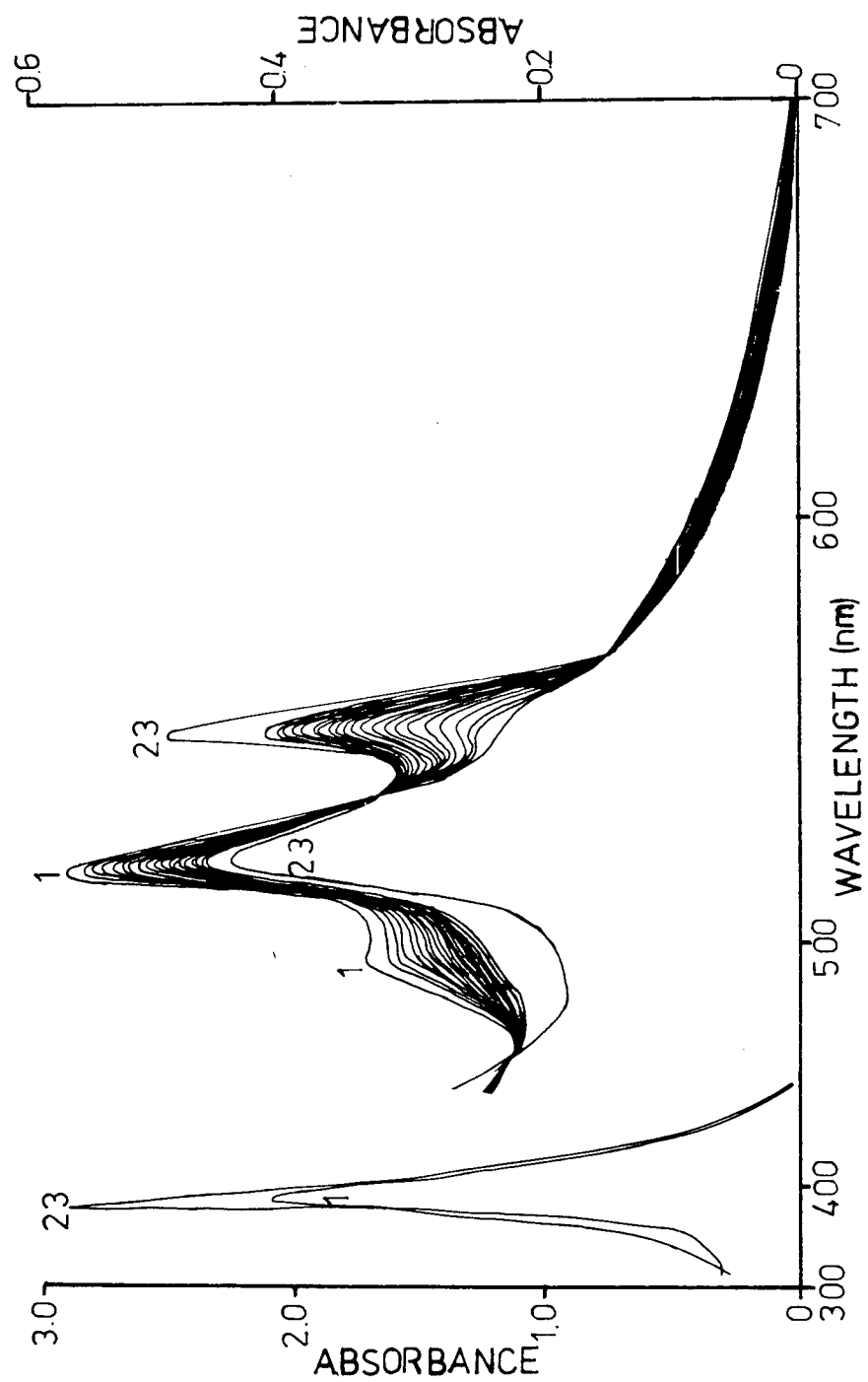
Figure V.12. Spectral Changes for the Reaction of Species 'Y' with 1 atm CO in pyrrole at 30°C.
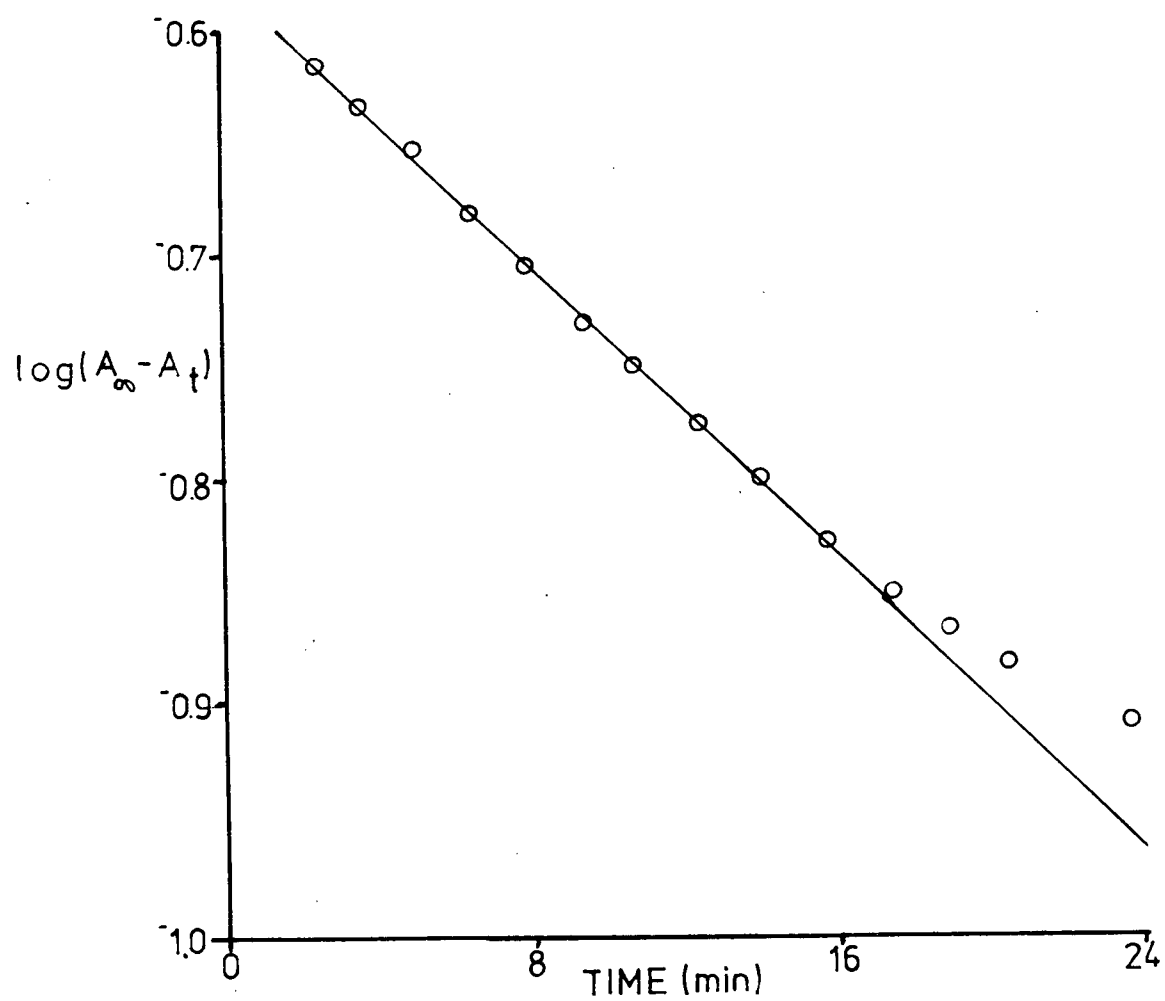
Figure V.13. First-Order Plot of the Reaction of Species 'Y' with 1 atm CO in pyrrole at $30^\circ C$.

about one ½-life, the plot curves away from linearity. For a first-order reaction, the log plot is normally linear for at least 3 half-lives. Again the reaction does not seem to be a simple equilibrium as exemplified in equation 20, even though good isosbestic points were obtained throughout the reaction.

$$RuOEP(L)(L') + CO \overset{K}{\rightleftharpoons} RuOEP)(CO)L(or~L') + L'~(or~L) \tag{20}$$

where L and L' can be pyrrole and/or acetonitrile.

The data could result from CO reacting with two different species present in solution at different rates (cf. eq. 20), one species reacting much more slowly and this could complicate the kinetics. Some sort of rearrangement could also be occurring but the spectrum of the reaction product is similar to RuOEP(CO)(pyrrole) so this is doubtful. Again, more work must be done to straighten out the problems of what are the species in solution.

CHAPTER 6

CONCLUSIONS

In the case of $RuOEP(CH_3CN)_2$ in toluene, excess acetonitrile was needed in order to stabilize the six-coordinate $RuOEP(CH_3CN)_2$ species in solution. Under these conditions at $30^\circ C$, in all cases, the reaction with up to 1 atmosphere CO went to completion giving $RuOEP(CO)(CH_3CN)$ via a dissociative mechanism:

$$RuOEP(L)_2 \underset{k_{-1}}{\overset{k_1}{\rightleftharpoons}} RuOEP(L) \underset{k_{-2}}{\overset{k_2}{\rightleftharpoons}} RuOEP(CO)L \qquad (21)$$
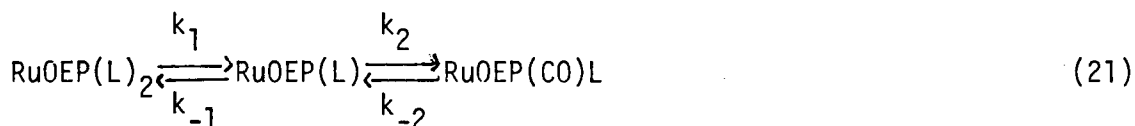
With the $L = P(n-Bu)_3$ system in toluene, no excess phosphine was necessary to maintain the six-coordinate species which, under these conditions, reacted with CO to fully form the carbonyl. However, in order to do kinetic studies on this system, excess phosphine was necessary to maintain pseudo-first-order kinetics. Under these conditions, the reaction of $RuOEP(P(n-Bu)_3)_2$ with 1 atm CO gave an equilibrium mixture with $RuOEP(CO)(P(n-Bu)_3)$, the CO being easily displaced by the excess of phosphine ligand.

Kinetic and thermodynamic parameters are presented for both systems $(L = CH_3CN, P(n-Bu)_3)$, and the data compared within the systems and with those for some Fe(II)(porphyrin) systems. Based on the k_{-1}/k_2 values for these M(porphyrin)L_2 species, a hypothesis as to the structure of

the corresponding five-coordinate intermediate was made, which suggests, for the $RuOEP(CH_3CN)$ and $RuOEP(P(n-Bu)_3)$ intermediates, that the metal centres are more in the porphyrin plane than out of it.

The $RuOEP(CH_3CN)_2$ complex in toluene also binds both N_2 and C_2H_4, but the systems proved difficult to study, one factor being the extreme photosensitivity of the products, the coordinated gas molecules being photolabile.

When $RuOEP(CH_3CN)_2$ was dissolved in coordinating solvents (py, DMA, DMF, THF and pyrrole), the anticipated $RuOEP(solvent)_2$ species was formed only in pyridine. However, $RuOEP(py)_2$ does not react with 1 atm CO in neat pyridine; on diluting the pyridine with toluene, a slow partial reaction occurs to give the monocarbonyl, $RuOEP(CO)(py)$.

On dissolution of solid $RuOEP(CH_3CN)_2$ in DMA, DMF or THF, the spectrum achieved is not that of the $RuOEP(solvent)_2$ species, which can be formed in situ by the photolysis of $RuOEP(CO)(EtOH)$ in the solvent; the much broader visible spectrum is believed to be that of $RuOEP(CH_3CN)(solvent)$, species 'X'. This species 'X' can be photolyzed to give $RuOEP(solvent)_2$ which slowly reverts back thermally to species 'X'. Species 'X' reacts with CO to give an instantaneous spectral change, followed by slower changes, that suggest that $RuOEP(CO)(solvent)$ is being formed. The sudden spectral change is tentatively suggested to involve a decarbonylation of the solvent to give, for example with DMA, $RuOEP(CO)(N(CH_3)_3)$; the subsequent slow reaction could be replacement of the amine by the solvent.

In the case of dissolution of the bis(acetonitrile) complex in pyrrole, again the initial spectrum is not that of the $RuOEP(pyrrole)_2$ species. Reaction with CO gives a series of spectral changes to give what

appears to be RuOEP(CO)(pyrrole). However, a first-order kinetic plot
of this reaction is only linear for about one half-life. Perhaps two
species, RuOEP(CH$_3$CN)(pyrrole) and RuOEP(pyrrole)$_2$, are present in solution
and they react with CO at different rates.

The presence of the acetonitrile ligands (initially chosen to be an
innocent ligand in strongly coordinating solvents) is having a pronounced
effect on the chemistry of the RuOEP species. A major problem in studying
these systems, is that most RuOEP(L)(L') complexes show visible and Soret
bands at wavelengths that are independent of L, thus making identification
of the species in solution difficult. One worthwhile effort would be
isolation of other RuOEP(L)$_2$ species, for example, with L = DMA, DMF,
THF and pyrrole.

REFERENCES

1.   B. R. James, in 'The Porphyrins', D. Dolphin, Ed., Vol. V, Academic Press, New York, 1978, p. 205.

2.   R. W. Erskine and B. O. Field, Struct. Bonding, 28, 1 (1976).

3.   G. McLendon and A. E. Martell, Coord, Chem. Rev., 19, 1 (1976).

4.   L. Vaska, Acc. Chem. Res., 9, 175 (1976).

5.   J. P. Collman, Acc. Chem. Res., 10, 265 (1977).

6.   J. W. Buchler, Angew. Chem. Int. Ed. Engl., 17, 407 (1978).

7.   T. G. Traylor, in 'Bioorganic Chemistry', E. E. Van Tamelen, Ed., Vol. IV,   Academic Press, New York, 1978, p. 437.

8.   R. D. Jones, D. A. Summerville and F. Basolo, Chem. Rev., 79, 139 (1979).

9.   J. P. Collman, R. R. Gagne, C. A. Reed, W. T. Robinson and G. A. Rodley, Proc. Natl. Acad. Sci. USA., 71, 1326 (1974).

10 (a).   M. F. Perutz, Nature (London), 228, 726 (1970).

   (b).   M. F. Perutz, Nature (london), 237, 495 (1972).

   (c).   M. F. Perutz, Ann. Rev. Biochem., 48, 327 (1979).

11.   M. F. Perutz, Nature (London), 228, 283 (1965).

12 (a).   B. M. Hoffman, C. A. Petering, Proc. Natl. Acad. Sci. USA., 67, 637 (1970).

   (b).   J. P. Collman, R. R. Gagne, J. Kouba and H. Ljusgerg-Wagren, J. Am. Chem. Soc., 96, 6800 (1974).

   (c).   H. Yamamoto. T. Takayangi, T. Kwan and T. Yonetani, Bioinorg. Chem., 7, 189 (1977).

   (d).   D. W. Smith, PhD. Thesis, U.B.C., Vancouver, B.C. (1980).

13 (a).   B. M. Hoffman, C. J. Weschler and F. Basolo, J. Am. Chem. Soc., 98, 5473, (1976).

   (b).   R. D. Jones, D. A. Summerville and F. Basolo, J. Am. Chem. Soc., 100, 4416 (1978).

14.   J. M. Latour, J. C. Marchon and N. Nakajima, J. Am. Chem. Soc., 101, 3974 (1979).

15 (a). B.R. James and D V. Stynes, J. Am. Chem. Soc., 94, 6225 (1972).

   (b). B. B. Wayland and A. R. Newman, J. Am. Chem. Soc., 101, 6472 (1979).

16.   A. H. Corwin and R. Reyes, J. Am. Chem. Soc., 78, 2437 (1956).

17.   D.-H. Chin, G. N. LaMar and A. L. Balch, J. Am. Chem. Soc., 102, 4344 (1980).

18 (a). E. B. Fleischer, Acc. Chem. Res., 3, 105 (1970).

   (b). H. Gray, Adv. Chem. Ser., 100, 365 (1971).

19.   M. Gerloch, E. D. McKenzie and A. D. C. Towl, J. Chem. Soc. A, 2850 (1969).

20.   F. Basolo, B. M. Hoffman and J. Ibers, Acc. Chem. Res., 8, 384 (1975).

21.   J. H. Wang, J. Am. Chem. Soc., 80, 3168 (1958).

22.   C. K Chang and T. G. Traylor, Proc. Nat'l. Acad. Sci. USA., 70, 2647 (1973).

23 (a). C. K. Chang and T. G. Traylor, Proc. Nat'l. Acad. Sci. USA., 72, 1166 (1975).

   (b). G. C. Wagner and R. J. Kassner, J. Am. Chem. Soc., 96. 5593 (1974).

   (c). D. L. Anderson, C. J. Weschler and F. Basolo, J. Am. Chem. Soc., 96, 5257 (1974).

   (d). J. Almog. J. E. Baldwin, R. L. Dyer, J. Huff and C. J. Wilkerson, J. Am. Chem. Soc., 96, 9600 (1979).

24.   J. E. Baldwin and J. Huff, J. Am. Chem. Soc., 95, 5257 (1973).

25 (a). J. P. Collman, J. I. Brauman, K. M. Doxsee, T. R. Halbert, E. Bunnenberg, R. E. Linden, G. N. LaMar, J. Del Gaudio, G. Lang and K. Sparlatian, J. Am. Chem. Soc., 102, 4182 (1980).

   (b). J. P. Collman, R. R. Gagne, T. P. Halbert, J.-C. Suslick and C. A. Reed, J. Am. Chem. Soc., 95, 7868 (1973).

26.   J. P. Collman, J. I. Brauman, E. Rose and K. S. Suslick, Proc. Nat'l. Acad. Sci. USA., 75, 1052 (1978).

27 (a). G. B. Jameson, G. A. Rodley, W. T. Robinson, R. R. Gagne, C. A. Reed and J. P. Collman, Inorg. Chem., 17, 850 (1978).

   (b). G. B. Jameson, F. S. Molinaro, J. A. Ibers, J. P. Collman, J. I. Brauman, E. Rose and K. S. Suslick, J. Am. Chem. Soc., 100, 6769 (1978).

28. D. V. Stynes and B. R. James, J. Am. Chem. Soc., 96, 2733 (1974).

29. C. J. Weschler, D. L. Anderson and F. Basolo, J. Am. Chem. Soc., 97, 6707 (1975).

30. B. R. James, K. J. Reimer and C. T. Wong, J. Am. Chem. Soc., 99, 4815 (1977).

31. N. Farrell, D. H. Dolphin and B. R. James, J. Am. Chem. Soc., 100, 324 (1978).

32. D. R. Paulson, A. W. Addison, D. H. Dolphin and B. R. James, J. of Biol. Chem., 254, 7002 (1979).

33. D. F. Shriver, 'The Manipulation of Air Sensitive Compounds', McGraw-Hill, New York, N. Y., 1969.

34. M. Tsutsui, D. Ostfeld, J. N. Francis and L. M. Hoffman, J. of Coordination Chem., 1, 115 (1971).

35. F. R. Hopf, T. P. O'Brien, W. R. Scheidt and D. G. Whitten, J. Am. Chem. Soc., 97, 277 (1975).

36. B. R. James, A. W. Addison, D. Dolphin, D. R. Paulson, J. Biol. Chem., 254, 2082 (1979).

37. A. Seidell, 'Solubilities of Inorganic and Metal Organic Compounds', Vol 1, 3rd ed, D. Van Nostrand Co., New York, N. Y., 1970, p 218.

38. B. R. James, D. Dolphin and N. Farrell, unpublished results.

39. B. R. James, A. W. Addison, M. Cairns, D. Dolphin, N. P. Farrell, D. R. Paulson and S. Walker, Fundam. Res. Homogeneous Catal., 3, 571 (1979).

40. D. V. Stynes and B. R. James, J. Chem. Soc., Chem. Comm., 325 (1973).

41. G. Hammond, J. Am. Chem. Soc., 77, 334 (1955).

42. L. J. Radonovich, A. Bloom and J. L. Hoard, J. Am. Chem. Soc., 94, 2073 (1972).

43. I. Amdur and G. G. Hammes in 'Chemical Kinetics, Principals and Selected Topics', McGraw-Hill, New York, N. Y., 1962, p 12.

44. B. R. James and R. LeBlanc, work in progress.

45. W. A. G. Graham, Inorg. Chem., 7, 315 (1968).

46. B. R. James, D. Dolphin, B. Tarpey and G. Domazetis, Chem. Comm., in press.

47. F. R. Hopf and D. C. Whitten, J. Am. Chem. Soc., 98, 7422 (1976).

48. A. D. Allen, T. Eliades, R. O. Harris and P. Reinsatu, Canad. J. Chem., 47, 1605 (1969).

49. D. A. Summerville, T. W. Cape, E. D. Johnson and F. Basolo, Inorg. Chem., 17, 3297 (1978).

50. L. Vaska, Acc. Chem. Res., 1, 335 (1968).

51. W. H. Knoth, J. Am. Chem. Soc., 90, 7172 (1968).

52. A. Anitpas, J. W. Buchler, M. Gouterman and P. D. Smith, J. Am. Chem. Soc., 100, 3015 (1978).

53. D. J. Cole-Hamilton and G. Wilkinson, Chem. Comm., 883 (1978).

54. G. R. Eaton and S. S. Eaton, J. Am. Chem. Soc., 97, 235 (1975).

55. B. R. James and R. LeBlanc, unpublished results.

56. B. R. James, Inorg. Chim. Acta. Rev., 4, 73 (1970).

57. S. A. Fouda, B. C. Y. Hui and G. L. Rempel, Inorg. Chem., 17, 3213 (1978).

58. A. Rusoa and A. A. Vlček, Nature, 206, 295 (1965).